Spatial patient registration in robotic neurosurgery

Šuligoj, Filip

Doctoral thesis / Disertacija

2018

Degree Grantor / Ustanova koja je dodijelila akademski / stručni stupanj: **University of Zagreb, Faculty of Mechanical Engineering and Naval Architecture / Sveučilište u Zagrebu, Fakultet strojarstva i brodogradnje**

Permanent link / Trajna poveznica: https://urn.nsk.hr/urn:nbn:hr:235:555139

Rights / Prava: In copyright / Zaštićeno autorskim pravom.

Download date / Datum preuzimanja: **2024-03-29**

Repository / Repozitorij:

Repository of Faculty of Mechanical Engineering and Naval Architecture University of Zagreb







Sveučilište u Zagrebu

FACULTY OF MECHANICAL ENGINEERING AND NAVAL ARCHITECTURE

FILIP ŠULIGOJ

SPATIAL PATIENT REGISTRATION IN ROBOTIC NEUROSURGERY

DOCTORAL THESIS

Zagreb, 2018



Sveučilište u Zagrebu

FAKULTET STROJARSTVA I BRODOGRADNJE

FILIP ŠULIGOJ

PROSTORNA REGISTRACIJA PACIJENTA U ROBOTSKOJ NEUROKIRURGIJI

DOKTORSKI RAD

Zagreb, 2018



Sveučilište u Zagrebu

FACULTY OF MECHANICAL ENGINEERING AND NAVAL ARCHITECTURE

FILIP ŠULIGOJ

SPATIAL PATIENT REGISTRATION IN ROBOTIC NEUROSURGERY

DOCTORAL THESIS

SUPERVISOR:

Prof.dr.sc. Bojan Jerbić

Zagreb, 2018



Sveučilište u Zagrebu

FAKULTET STROJARSTVA I BRODOGRADNJE

FILIP ŠULIGOJ

PROSTORNA REGISTRACIJA PACIJENTA U ROBOTSKOJ NEUROKIRURGIJI

DOKTORSKI RAD

Mentor:

Prof.dr.sc. Bojan Jerbić

Zagreb, 2018

BIBLIOGRAPHY DATA

Scientific area: TECHNICAL SCIENCES

Scientific field: Mechanical engineering

Institution: Faculty of Mechanical Engineering and Naval Architecture

Thesis supervisor: Prof.dr.sc. Bojan Jerbić

*Number of pages:*113

*Number of figures:*16

*Number of tables:*4

*Number of references:*100

Date of public defence:

Thesis committee:

Prof. dr. sc. Andrej Jokić, Associate Professor, Chairman of the thesis committee

Prof. dr. sc. Bojan Jerbić, Full Professor, Thesis supervisor

Prof. dr. sc. Darko Chudy, MD, Assistant Professor, – External member

Archive: Faculty of Mechanical Engineering and Naval Architecture

TABLE OF CONTENTS

Preface IV
Acknowledgement V
Summary VI
Sažetak VII
Proširenи sažetak VIII
Ključne riječi XI
Keywords XII
List of abbreviations XIII
Nomenclature XIV
List of Figures XVI
List of Tables XVII
1 Introduction 1
1.1 Background 1
1.2 Robot image-guided interventions 3
1.3 Robotics in neurosurgery 4
1.3.1 State of the art in robotic patient registration 5
1.3.2 State-of-the-art methods for localization in medical images 6
1.4 RONNA – RObotic NeuroNavigAtion 7
1.5 Research motivation 10
1.6 Objective and hypotheses of the research 11
1.7 Scientific contribution 11
2 Registration 12
2.1 Mathematical background 12
2.2 Registration methods and algorithms 15
2.3 Correspondence problem 17
2.4 Singular Value Decomposition (SVD) 18
3 Patient localization 20
3.1 Image space localization 20
3.2 Physical space localization 21
4 Error analysis 23
4.1 Measures of localization and registration errors 23

4.2 Error analysis of a neurosurgical robot system 25
5 Selected results and discussion 27
5.1 Automated localization in the image space 27
5.2 Framework for the automated patient registration procedure 30
5.3 Correspondence algorithm 32
5.3.1 Testing of the correspondence algorithm in a simulated point environment 34
5.3.2 Testing of the correspondence algorithm on clinical data 35
5.4 Robot localization strategy and the accuracy of the neurosurgical robot system 37
6 Conclusions and future work 41
7 Literature 44
8 Curriculum vitae 50
9 Summary of papers 53
10 Appendix 58
Paper 1 59
Paper 2 70
Paper 3 76
Paper 4 90
Paper 5 101

PREFACE

Sapienta ducet ad astra

Wisdom leads to the stars

ACKNOWLEDGEMENT

The work presented in this thesis was carried out at the Department of Robotics and Production System Automation of the Faculty of Mechanical Engineering and Naval Architecture, University of Zagreb.

First, I would like to express gratitude to my supervisor and mentor, Professor Bojan Jerbić, who gave me the opportunity to work in his group and who has supported me throughout my academic career and in the process of writing this thesis. His mentoring was always at the highest level, helpful and highly motivational.

I would also like to thank sincerely the thesis committee members, prof. dr. sc. Andrej Jokić, Associate Professor, and prof. dr. sc. Darko Chudy, Assistant Professor, MD, for their input, comments, and advice.

I would also like to show my gratitude to all dear colleagues at the Department of Robotics and Production System Automation, teams from the Clinical Hospital Dubrava and the projects NERO and FAT for helpful discussions and a friendly atmosphere.

A big thank you to my closest and dearest colleagues Marko, Bojan, and Josip for good joint work in general and on the project RONNA, which is deeply engraved in this doctoral thesis. Bojan and Marko, I had been lucky enough in life to be able to call you my friends long before we became colleagues and I hope that this will never change.

I feel deep and sincere gratitude to my family for their love, help, and support. I am forever indebted to my parents for giving me the opportunities that have made me who I am. This journey would not have been possible if it had not been for them, and I dedicate this milestone to them.

Finally, I thank Maja and Maša, my wife and daughter, with all my love. The endless love I feel towards both of you makes me a better person. Maja has been my best friend and has loved, supported, encouraged, and helped me rise to all the challenges of life in the most positive way.

SUMMARY

In medicine, robots can be applied as a part of complex and computer-assisted systems for diagnosis, preoperative planning, surgery, post-operative patient care, and hospital logistics. Surgical robot systems can improve the existing operative procedures in terms of better efficiency, accuracy, and greater reliability of performance. Since the operating target in neurosurgery is not visible, the use of robots requires spatial patient registration. The spatial patient registration is an alignment of patient images acquired by means of an appropriate kind of scan technology with a patient located in the operating room (OR). Registration, in general, is a fundamental problem which occurs in many scientific fields, such as machine vision, image processing, robotics, and medicine, and it denotes transformation of two data sets into one coordinate system.

The research proposed in this doctoral thesis addresses major elements of spatial patient registration in robotic neurosurgery: localization of the patient in the medical images and in the OR, rigid point-based registration, and automation of the overall patient registration procedure. This implies a good knowledge of the state-of-the-art methods in robotic surgery, the development and implementation of new methods and algorithms, and measurements that evaluate the achieved results. In order to improve the image space localization, a novel algorithm was developed; it uses a unique approach combining machine vision algorithms, biomedical image filtration methods, and mathematical estimation methods to determine the centre of each individual fiducial marker. A novel correspondence algorithm and a framework for an automatic patient registration procedure using freely distributed fiducial markers in the application of a robot in neurosurgery were established. Both the image space and the physical space localization, and, subsequently, the registration, are executed autonomously and do not require the additional employment of the medical personnel. For localization in the physical space, a concept of robot localization strategy was introduced, implemented, and tested. Localization strategies use specific approach angles, orientations and types of movement of a robot during the fiducial marker localization procedure in the physical space and positioning to the target points. Influence of the robot localization strategy on the overall application error of a robot system used in frameless stereotactic neurosurgery was measured and analysed.

SAŽETAK

U interventnoj medicini, roboti se općenito mogu primijeniti kao dio kompleksnih i računalno potpomognutih sustava koji imaju mogućnosti dijagnoze, predoperativnog planiranja, provođenja operativnih zahvata, postoperativne njege, vođenja bolničke logistike itd. Kirurški robotski sustavi mogu unaprijediti postojeće operativne procedure poboljšanom efikasnošću, preciznošću i većom sigurnošću izvođenja. Budući da operativni ciljevi u neurokirurgiji u većini slučajeva nisu vidljivi, upotreba robota zahtijeva prostornu registraciju pacijenta. Prostorna registracija pacijenta podrazumijeva povezivanje snimaka pacijenta dobivenih odgovarajućom tehnikom skeniranja s pacijentom smještenim u operacijskoj sali. Registracija je temeljni problem koji se pojavljuje u mnogim znanstvenim područjima kao što su strojni vid, obrada slike, robotika i medicina te označava transformaciju dvaju skupa podataka u jedan koordinatni sustav.

Istraživanje predloženo u ovom doktorskom radu obrađuje glavne komponente prostorne registracije pacijenta u robotskoj neurokirurgiji: lokalizaciju pacijenta u medicinskim snimkama i operacijskoj sali, krutu (eng. rigid) registraciju i automatizaciju cjelokupnog postupka prostorne registracije pacijenata. Podrazumijeva se dobro poznavanje suvremenih metoda primjenjenih u robotskim medicinskim zahvatima, razvoj i implementacija novih metoda i algoritama te mjerenja na temelju kojih se mogu vrednovati postignuti rezultati. Kako bi se poboljšala lokalizacija pacijenta u volumetrijskim snimkama razvijen je novi algoritam koji koristi jedinstven pristup odnosno kombinaciju algoritama strojnog vida, biomedicinskih metoda filtriranja slike i metoda matematičke procjene kako bi se utvrdilo središte svakog markera. Razvijen je algoritam za uparivanje točaka i sustav za automatsku registraciju pacijenta koji koristi slobodno distribuirane markere. Lokalizacija u medicinskim snimkama i fizičkom prostoru, a potom i registracija, odvijaju se samostalno te ne zahtijevaju dodatnu intervenciju medicinskog osoblja. Za lokalizaciju u fizičkom prostoru je predstavljen, implementiran i testiran koncept strategije robotske lokalizacije. Lokalizacijske strategije koriste specifične kuteve, orijentacije i vrste kretanja robota tijekom postupka lokalizacije markera i pozicioniranja na ciljanu točku. Izmjereni su i analizirani utjecaji strategije robotske lokalizacije na ukupnu pogrešku robotskog sustava za stereotaktičku neurokirurgiju.

PROŠIRENI SAŽETAK

Roboti kao fizička manifestacija računala služe rasterećenju čovjeka od teških i monotonih poslova. Primjenjuju se u industrijskoj proizvodnji, kontroli kvalitete, automatizaciji laboratorijskih procesa, nadzoru, različitim uslužnim djelatnostima, ali i u medicini. U interventnoj medicini, roboti se općenito mogu primijeniti kao dio kompleksnih i računalno potpomognutih sustava koji imaju mogućnosti dijagnoze, predoperativnog planiranja, provođenja operativnih zahvata, postoperativne njege, vođenja bolničke logistike itd. Kirurški robotski sustavi mogu unaprijediti postojeće operativne procedure poboljšanom efikasnošću, preciznošću i većom sigurnošću izvođenja.

Snimkom navođene intervencije IGI (eng. Image guided interventions) [1] kirurški je koncept u kojem se koriste snimke magnetske rezonance (MR), računalne tomografije (CT), rentgenskog snimanja (RTG), kompjutorizirane i pozitronske tomografije (PET/CT i SPECT/CT) i ostalih radioloških metoda. Dobivene trodimenzionalne (3D) informacije o ljudskoj anatomiji koriste se za predoperativno planiranje, vizualizaciju unutarnjih struktura ljudskog tijela i navođenje kirurških instrumenata za vrijeme zahvata. Navedene metode koriste se u kliničkim primjenama poput neurokirurgije, kardiokirurgije i ortopedske kirurgije. Neuronavigacijski sustavi su standardna metoda u IGI. Glavna razlika između neuronavigacijskih i robotskih sustava očituje se u operativnoj fazi gdje se robot kao pogonjeni sustav može kretati neovisno od kirurga, dok neuronavigacija samo prati i prikazuje položaj alata u odnosu na snimku pacijenta. Opća procedura IGI sastoji se od sljedećeg niza koraka: predoperativno snimanje pacijenta, predoperativna vizualizacija i planiranja intervencije, registracija pacijenta i navođenje kirurškog instrumenta. U predoperativnoj fazi kirurg koristi radiološke snimke pacijenta za vizualizaciju i planiranje intervencije. Proces registracije u kontekstu strojnog vida podrazumijeva poklapanje različitih slika istog objekta iz različitih pogleda i u različito vrijeme [2]. Osnovne tri komponente registracije su: transformacija između izvornih i konačnih slika, mjera sličnosti između slika i optimizacija koja određuje najbolje transformacijske parametre. Medicinska registracija pacijenta podrazumijeva određivanje transformacije između različitih vrsta radioloških snimaka ili pak transformacije između radiološke snimke i pacijenta u fizičkom prostoru [3]. Lokalizacija je proces pronalaska značajki od interesa, a provodi se odvojeno u radiološkim snimkama i u fizičkom prostoru. Lokalizacija pacijenta u radiološkim snimkama znači određivanje pozicije značajki u koordinatnom sustavu uređaja za snimanje. Lokalizacija pacijenta u fizičkom

prostoru označava određivanje njegove pozicije u koordinatnom sustavu uređaja kojim se lokalizira u operacijskoj sali. Značajke koje se koriste za lokalizaciju pacijenta mogu biti anatomske strukuture pacijenta ili vanjski objekti koji se pričvršćuju na pacijenta poput stereotaktičkog okvira, markera vijčano pričvršćenih za kost i ljepljivih markera. U stvarnim situacijama pogreške u lokalizaciji posljedica su šuma na senzorima, pogrešaka uzrokovanih diskretizacijom ulaznog signala i razlučivosti samog uređaja što utječe na točnost registracije. U studiji [4], testirano je sedam različitih metoda registracije temeljem in vivo mjerenja na trideset pacijenata. U usporedbi s drugim metodama registracije, metode s krutim markerima pričvršćenim na kost pokazale su najviše izmjerene točnosti jer nisu podložne pomicanju kože. Mjera nepoklapanja transformacije u fazi registracije povećava grešku pozicioniranja kirurškog instrumenta u planiranu poziciju. Steinmeier [5] je koristio akrilni fantom i dva različita neuronavigacijska sustava (StealthStation, Medtronic USA i Zeiss MKM, Carl Zeiss, Oberkochen, Germany) kako bi testirao utjecaj različitih faktora na grešku pozicioniranja alata. U zaključku istraživanja navedeno je da točnost neuronavigacijskih sustava najviše ovisi o procesu registracije. Uz samu točnost sustava, velika važnost pridodaje se i mogućnosti pouzdane procjene greške u specifičnim operacijama, kako bi se uklonio rizik od zahvaćanja kritičnih operativnih područja.

Cilj i hipoteza

Cilj istraživanja je razvoj matematičkih metoda i računalnih algoritama za prostornu registraciju pacijenta u robotskoj neurokirurgiji. Budući da prostorna registracija uključuje lokalizaciju pacijenta u radiološkim snimkama, kao i fizičkom prostoru, predloženo rješenje treba omogućiti dvosmjernu verifikaciju lokaliziranih značajki i procjenu greške registracije.

Hipoteze istraživanja:

1) Automatsko pronalaženje lokalizacijskih značajki u 3D prostoru radioloških snimaka moguće je postići estimacijom njihovog geometrijskog težišta na temelju specifičnih oblikovnih struktura identificiranih korištenjem algoritama strojnog vida u 2D presjecima.

2) Problem uparivanja lokaliziranih točaka i uklanjanje krivih očitanja moguće je riješiti analizom razlika udaljenosti parova točaka i distribucije grešaka mjernih uređaja.

Znanstveni doprinos

Rezultati ovog istraživanja kao i izvorni znanstveni doprinos su:

- razvijen inovativan algoritam za prepoznavanje lokalizacijskih značajki u CT snimkama pacijenata;
- rješenje problema uparivanja lokaliziranih točaka sa svrhom povećanja stupnja automatizacije i pouzdanosti prostorne registracije pacijenta;
- model za procjenu točnosti pozicioniranja robota na temelju registracije pogreške.

KLJUČNE RIJEČI

Medicinska robotika

Registracija

Obrada biomedicinskih slika

Algoritam za uparivanje točaka

Robotska lokalizacija

Točnost

RONNA

KEYWORDS

Medical robotics

Registration

Biomedical image processing

Correspondence algorithm

Robot localization

Accuracy

RONNA

LIST OF ABBREVIATIONS

1D	One-dimensional
2D	Two-dimensional
3D	Three-dimensional
CAD	Computer-aided design
CAS	Computer-assisted surgery
CT	Computed tomography
DOF	Degree of freedom
FLE	Fiducial localization error
FRE	Fiducial registration error
IGI	Image-guided interventions
MRI	Magnetic resonance imaging
OR	Operating room
OTS	Optical tracking system
PET/CT	Positron-emission tomography/computed tomography
RIGI	Robot image-guided interventions
RMS	Root-mean-square
ROI	Region of interest
SAD	Sum of absolute differences
SF	Stereotactic frame
SPC	Simultaneous pose and correspondence problem
SPECT	Single-photon emission computed tomography
SSD	Sum of squared differences
SVD	Singular value decomposition
TCP	Tool centre point
TPE	Target positioning error
TRE	Target registration error

NOMENCLATURE

$\mathbb{R}$	the real numbers
n, N	number of points
$\mathbf{p}_i$	the i-th point
$\mathbf{p'}_i$	the i-th point after transformation
$\mathbf{p''}_i$	the i-th point after two transformations
a, b	translation vector
$\mathbf{T_a}$	translation matrix for the vector **a**
T	translation matrix
t	translation vector
R, Q	rotation matrix
M	transformation matrix
q_i	the i-th parameter that defines transformation
A, B, C	matrix
U	$m \times m$ orthogonal matrix;
V	$n \times n$ orthogonal matrix;
S	diagonal matrix with singular values
Ω	set of orthogonal rotation matrices
$\mathbf{x}_i$, $\mathbf{y}_j$	coordinates of the i-th point in a set
$\widehat{\mathbf{x}_i}$, $\widehat{\mathbf{y}_j}$	true point coordinates
$\mathbf{e}_{\mathbf{x}i}$, $\mathbf{e}_{\mathbf{y}j}$	point localization errors
$\{\mathbf{x}_i\}$	set of points
$\{\mathbf{y}_i\}$	set of points
$\bar{\mathbf{x}}$	average value of the set $\{\mathbf{x}_i\}$
$\bar{\mathbf{y}}$	average value of the set $\{\mathbf{y}_i\}$
det(**A**)	determinant of the matrix **A**
$\mathbf{q}_j$	position of a j-th fiducial in the image space
$\mathbf{p}_j$	position of a j-th fiducial in the physical space
M	number of different registrations
d_k	minimal distance of a point from the k-th principal axis
f_k	RMS distance of the fiducials from the k-th axis
$\mathbf{e}^{\mathrm{app}}$	vector of application error
$\|\mathbf{e}^{\mathrm{app}}\|$	magnitude of the robot system application error

$\mathbf{e}^{\mathrm{reg}}$	registration error
$\mathbf{e}^{\mathrm{intr}}$	robot intrinsic error
$\mathbf{p}^{\mathrm{reg}}$	point which is transformed in the registration procedure
$\mathbf{p}^{\mathrm{true}}$	true position of **p**
$\mathbf{p}^{\mathrm{reached}}$	actual position the robot tool has reached
$\boldsymbol{\theta}$	vector containing six joint angles that define the position of a 6DOF robot
θ_i	angle of the *i*-th robot joint
${}_2^1\mathbf{A}\cdot$	transformation between the coordinate systems 1 and 2

LIST OF FIGURES

(Research paper figures not included)

Figure 1. s) The RONNA system (render) b) The RONNA system with components: (A) Master robot, (B) Assistant robot, (C) Universal mobile platform, (D) Optical tracking system, (E) Control and planning software interface .. 7
Figure 2. a) The bone-implanted x-shaped frame (a2) with four fiducial markers (a1); b) Freely distributed fiducial markers composed of: (b1) a self-drilling and self-tapping screw, (b2) a removable base, (b3) a retro-reflective sphere, i.e. a fiducial marker 9
Figure 3. Re-localization of fiducial markers by means of RONNAstereo..... 10
Figure 4. The SVD method results for known correspondence between point pairs [64]..... 16
Figure 5. An example of the principal component analysis (PCA) [64]..... 16
Figure 6. An example of the iterative closest point (ICP) method[64]..... 17
Figure 7. Series of axial CT head slices 21
Figure 8. Demonstration of the neurosurgical robot system positioning errors 25
Figure 9. Localized fiducial markers highlighted in a CT scan: a) x-shaped frame, b) Freely distributed markers 30
Figure 10. Coordinate systems and transformations used for achieving an automatic patient registration procedure 32
Figure 11. Example of the correspondence algorithm iterations 33
Figure 12. Coordinates from adhesive fiducial markers (highlighted green) are used for testing the correspondence algorithm: a) Patient 1, b) Patient 2, c) Patient 3 34
Figure 13. Results of testing the correspondence algorithm on simulated data: unsuccessful correspondence and the false-positive result 35
Figure 14. The success rate of the correspondence algorithm with the data from five CT scans of a laboratory phantom and OTS measurements..... 36
Figure 15. The success rate of the correspondence algorithm with the data from 12 patient CT scans and OTS measurements..... 36
Figure 16. Measurement results of all localization strategies 40

LIST OF TABLES

(Research paper tables not included)

Table 1. Overview of industrial robots used for neuronavigation since the year 2000. [18]..... 2
Table 2. Ground truth estimation of phantom fiducial localization error (FLE) 28
Table 3. Intra-modal estimation of phantom fiducial localization error (FLE) 29
Table 4. Measurement results of localization strategies 39

1 INTRODUCTION

1.1 Background

Robots, as physical expansions of computers, are used to relieve people of hard and monotonous tasks. Robots are used in industrial production, quality control, automation of laboratory processes, surveillance, service industry, and medicine. In medicine, robots can be used as a part of complex computer-assisted systems for diagnosis, preoperative planning, surgery, post-operative patient care, and hospital logistics. Surgical robot systems can improve the existing operative procedures in terms of better efficiency, accuracy, and greater reliability of performance.

Since its introduction into human neurosurgery by Spiegel and Wycis almost 70 years ago, the stereotactic frame has been used as a standard targeting method for functional intracranial procedures, biopsies, and deep brain stimulation [6]. With advances in image-guided neurosurgical procedures over the past 30 years, alternative methods of performing surgical interventions have become more widely used by neurosurgeons [7-10]. The first application of a robot in medicine was in the field of neurosurgery when an industrial robot, PUMA 200, was successfully used in a frame-based configuration for the brain biopsy procedure in 1985 [11]. There are a few reasons why the first application of robotic technology was in the field of neurosurgery. As noted in [12], the human brain is an organ which is uniquely suited for robotic applications. It is symmetrically confined within a rigid container (the skull), which offers the potential for accurate patient localization by a robotic or an external localization system.

One of the biggest obstacles to a widespread robotization of neurosurgical procedures is the total cost of robot systems which is still very high [13]. On the other hand, standard industrial robots come in a wide range of kinematic configurations (serial-link manipulators with six or seven revolute joints) and can meet specifications required for a wide variety of applications in neurosurgery. Table 1 gives an overview of standard industrial robots which have been implemented as part of commercial or research neuronavigation robot systems since the year 2000. The benefits of implementing industrial robots are that the research and the development of the robotic arm have been done by the robot manufacturer, which contributes

to a lower price of the whole system. Regarding strict medical regulations and standards which are pointed out in [14], an alternative to standard industrial robots are robot manipulators certified as medical devices. An example of that alternative is the newly developed medical lightweight robot Kuka LBR Med (KUKA, Augsburg, Germany). As presented by the KUKA Healthcare robotics division, the LBR Med lightweight robot will be tested in accordance with IEC 60601-1, the technical standards for the safety and effectiveness of medical electrical equipment. The robot will be distributed with CE marking for electromagnetic compatibility (IEC 60601-1-2:2014), which will ensure an even easier integration into medical devices. However, standard industrial robots that are incorporated in the AQRATE system (KB Medical SA, Lausanne, Switzerland) [15], the ROSA Spine (Medtech, Montpellier, France) [16], and the ROSA Brain (Medtech) [17] have obtained both the CE mark and the FDA approval. This fact confirms the medical applicability of standard industrial robots as part of medical devices (details are given in Table 1).

Table 1. Overview of industrial robots used for neuronavigation since the year 2000. [18]

System (project)	Selected papers	Robot Manufacturer	Model	RR* [mm]	Payload [kg]
ROSA Spine	[16]Lefranc and Peltier 2016 [19] Chenin et. at. 2016	Stäubli	TX60L	±0.030	2
Aqrate	[15] Patel 2016	KUKA	KR6 R700	±0.030	6
REMEBOT	Liu Yu-peng et al., 2016	Universal robots	UR5	±0.100	5
TIRobot	[20] Tian et al., 2016 [21] Tian, 2016	Universal robots	UR5	±0.100	5
not specified	[22] Faria et al., 2016	Yaskawa Motoman	MH5	±0.020	5
Active project	[23] Beretta et al., 2015	KUKA	LWR4+	±0.100	7
RONNA	[24] Jerbić et. al. 2015	KUKA	KR6R900	±0.030	6
	[18] Švaco et. al. 2017	KUKA	KR6R900	±0.030	6
ROSA Brain	[17] Lefranc et. al. 2014 [8] González-Martínez et. al. 2016	Mitsubishi	RV3SB	±0.020	3
ROBOCAST	[25] Comparetti et al., 2012	Adept	Viper s1300	±0.070	5
OrthoMIT	[26] Tovar-Arriaga et al., 2011	KUKA/DLR	LWR3	±0.150	14
Pathfinder	[27] Deacon et al., 2010 [12] Eljamel 2007	Adept	Viper s1300	±0.070	5
RobaCKa	[28] Eggers et al., 2005	Stäubli	RX90	±0.025	6
CASPAR	[29] Burkart et al., 2001	Stäubli	RX90	±0.025	6

*RR – Robot Repeatability

In the last two years, four innovative robotic neuronavigation systems have been developed based on standard industrial robots from KUKA [15], Stäubli [16] and Universal robots [20] [21] (details are given in Table 1). These systems are not included in the current state-of-the-art literature survey and review papers [30-33]; this demonstrates a very rapid development of the robotized neuronavigation medical field.

1.2 Robot image-guided interventions

Medical image-guided interventions (IGI) [34] use information acquired from preoperative medical imaging methods such as magnetic resonance imaging (MRI), computed tomography (CT), radiography, positron-emission tomography-computed tomography (PET/CT), and single-photon emission computed tomography (SPECT). The three-dimensional (3D) data of the human anatomy (patient in the image space) obtained using these methods are then used for the visualization of inner anatomical structures of the human body, preoperative planning, surgical target definition, and accurate surgical tool guidance. Preoperative medical imaging methods have been introduced into clinical application in neurosurgery, cardiac surgery, and orthopaedic surgery. Stereotactic frame (SF) is commonly used in medical practice when it is needed to determine a precise point of surgery based on MRI, CT or other medical imaging techniques. The frame is manually positioned to physically guide the surgeon's tool to the desired point in its own coordinate system. Another example of IGI is a neuronavigation system which uses an optical tracking system (OTS) to precisely track the three-dimensional position and orientation of the surgical instrument in relation to the patient. The connection between the coordinate systems is derived from patient images, imaging software, and patient registration procedure. Methods used in IGI are the foundation for the development and implementation of robots in surgical procedures. The information used in the phase of preoperative planning and the patient registration procedure is the same as that required in robot surgery. Unlike neuronavigation systems which track and visualize special tools in relation to the patient, the motor-actuated and computer controlled robot systems can autonomously move surgical tools and perform tasks. In most applications robot image-guided interventions (RIGI) are used to accurately position or to navigate surgical instruments to the specific targets planned by using patient images [35].

A general sequence of steps in RIGIs includes a preoperative patient image scanning, preoperative visualization and intervention planning, patient-to-image registration, and surgical tool guidance. A surgeon uses the images acquired in the preoperative phase for the

visualizing and planning of surgery targets. Patient-to-image registration is a prerequisite for guiding the surgical tool to the targets defined in the image space. In machine vision, the term "registration" implies the aligning of two images of the same environment or object, which can be captured from different viewpoints, using different devices at different times [2]. Three main components of registration are: transformation between the source and final images, a degree of similarity between the images, and the optimization method that determines the best transformation parameters. A process of registration in the context of medical patient registration implies the determination of a spatial transformation between different image modalities or a transformation between the patient in the image space and the patient in the physical space [3]. Input data for the registration are obtained through localization. Objects externally attached to the patient are called fiducial markers and their geometrical centres can be used as reference points for the localization and "image space-to-physical space" registration process. These reference points are also called fiducial points. Localization is the process of determining the position of fiducial points in the image space or the physical space. Fiducial points in localization can be associated with anatomical structures of the patient or external objects attached to the patient, such as the stereotactic frame, bone-attached markers, and adhesive markers. Markers that are used for obtaining fiducial points are called fiducial markers. The proportion of misalignment in registration reduces the accuracy of the surgical tool positioning to the planned target.

1.3 Robotics in neurosurgery

From the robotics point of view, many problems in minimally invasive neurosurgery, which uses small incisions, can be classified as rigid body transformations because the brain is confined within a rigid container (the skull); hence, the implementation of robot systems in neurosurgery is suitable. On the other hand, a classic approach or so-called open surgery, applies procedures that are performed through a large and open cut on skull cause leakage of brain liquor and consequently brain shift. Brain shift changes the spatial position of the brain and invalidates the patient-to-image registration based on preoperative imaging data. In such cases, only intraoperative imaging can provide reliable registration for robot application. This work is primarily oriented to minimally invasive neurosurgery and use of preoperative imaging.

The main features required from a neurosurgical robot system are precision, accuracy, short setup time, reliability, safety, flexibility, and simple usage. A common trait of most modern

medical robot systems and image-guided surgical procedures is the fact that they possess little autonomy or very few automated functions [36]. A great number of operations are still performed manually, which can be attributed to the unstructured work environment in the OR and to demanding safety requirements in robotic surgery. As the main subject of this doctoral thesis is patient registration in robotic neurosurgery, the following state-of-the-art chapters are focused on the localization and registration methods and their level of automation and accuracy.

1.3.1 State of the art in robotic patient registration

State-of-the-art robot systems intended for neurosurgery and their patient registration methods differ in regard to the patient localization features, localization techniques, sensors, and registration procedures employed. As shown by Widmann et al. in [37], registration based on paired points is still the gold standard in frameless stereotactic neurosurgery. Nevertheless, in a number of patient registration procedures using robot systems, corresponding points between the image and the physical space, either fiducial points or anatomical landmarks, need to be manually matched. This is a time-consuming process prone to errors. Cardinale et al. [38] evaluate the new Neuromate (Renishaw, Gloucestershire, UK) Neurolocate touch-free localization device and its clinical workflow. After an intraoperative 3D image has been obtained using the O-arm Surgical Imaging System, the centres of the Neurolocate fiducial markers need to be selected semi-automatically in multi-planar reconstructions within the planning software. In [39], Benedictis et al. reported on the ROSA Brain neuronavigation robotic assistant (Medtech, Montpellier, France) which can be used with two types of registration: fiducial marker registration using bone-attached markers and frameless surface-based registration (i.e. noncontact patient localization). The first procedure is based on the manual positioning of the robot tool centre point (mechanical pointer) within the implanted screws on the patient's skull. González-Martínez et al. [8] and Lefranc et al. [17] used the ROSA Brain neuronavigation robot system with the noncontact localization method utilizing a custom-built laser for measuring distance. The main drawback of this approach is that the initial alignment between the image space and the physical space is done by the operator, through the manual guidance of the robotic arm, pinpointing a series of anatomical landmarks previously localized by the operator in the image space. Kronreif et al. [40] demonstrated a miniature robotic assistant system, B-RobII, which is navigated by a certified neuronavigation device (VectorVision, BrainLAB AG, Germany) using a manual registration procedure based on paired points. Gerber et al. [41] presented a semiautomatic ball-in-cone positioning method

for the localization of fiducial markers in the physical space by using a novel surgical robot system with force feedback control. In [42], Meng et al. present an optically tracked robot system that utilizes a pointer tool and a patient reference frame in order to determine the correspondence between fiducial marker points in the physical and the image space. The same method of robotic guidance was used in our research [43]. Lin et al. [44] developed a neurosurgical robotic drilling and navigation system which utilizes manual localization of fiducial points in the physical space. In a pilot study [45], the patient's teeth were successfully used in markerless registration. The system displayed high accuracy in the real-time 3D image matching of stereo vision data and integral videography image derived from a CT scan.

1.3.2 State-of-the-art methods for localization in medical images

Methods for the localization of fiducial points in volumetric images can be manual, semi-automatic, and automatic. Manual localization is a general approach that involves human operators; it is used with different fiducial marker types and imaging technologies. Semi-automatic and automatic localization algorithms have been introduced to overcome the drawbacks of manual localization and to improve localization and registration accuracy results. A priori knowledge, such as physical features and intensity values of the marker, is often used for the localization of fiducial points.

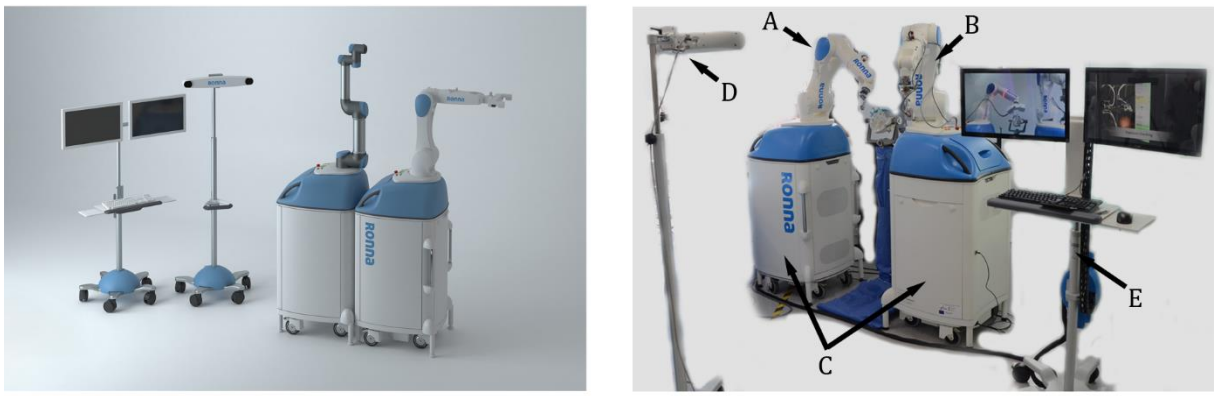
An example of semi-automatic localization is presented in [46]. First, the operator designates the rough location of the fiducial markers and then the algorithm localizes the fiducial points accurately using the intensity-based registration with mutual information similarity measure. As the authors point out, the advantage of such an approach is that it can be used for different types of fiducial markers and with different imaging modalities. Gerber et al. [41] developed a registration system for robotic microsurgery that localizes a screw in both the physical and the image space. Both methods use the semi-automatic approach for the coarse localization of the screw. Cropped sub-volumes of the image are used in this type of localization. The sub-volumes are selected by the operator and fitted to the surface of the 3D model of the screw. The robot uses a force-torque sensor for precise localization of the screw head in the physical space.

An automatic knowledge-based technique for localizing the centroids of cylindrical markers externally attached to the patient's head in the CT and the MR image volumes is presented in [47]. Machine vision algorithms are used to find the fiducial markers whose voxel intensities are higher than those of the surrounding space. Yaniv, [48, 49], uses externally placed spheres

for localization; we adopted a similar approach in our research [43]. When using a c-arm-based cone-beam CT (CBCT) instead of the localization in volumetric images, the method is able to provide coordinates of the fiducial markers from the projection images. The related research presented in [50] proposes a 3D surface modelling approach for the localization of spherical radio-opaque markers in CT scans. In that case, the optimized algorithm parameters deliver sub-millimetre localization accuracy with different CT resolutions. The performance of a block matching-based automatic registration algorithm is tested by Isamber et al. [51]. The accuracy of the process was measured for two different phantoms on CT, MR, and positron emission tomography (PET) images. The block matching-based algorithm yielded the below voxel accuracy.

1.4 RONNA – RObotic NeuroNavigAtion

A robotic neuronavigation system, RONNA, has been developed based on standard industrial robots by the research group from the Department of Robotics and Production System Automation, Faculty of Mechanical Engineering and Naval Architecture, University of Zagreb. The intended use of RONNA is stereotactic navigation. The basic version of the RONNA system has three main components: a robotic arm mounted on a universal mobile platform, a planning system, and a navigation system. The extended version of the RONNA system (shown in Figure 1.) consists of two robotic arms mounted on specially designed universal mobile platforms, a global optical tracking system (OTS), and a control and planning software interface.



a) b)

Figure 1. s) The RONNA system (render) b) The RONNA system with components: (A) Master robot, (B) Assistant robot, (C) Universal mobile platform, (D) Optical tracking system, (E) Control and planning software interface

The robots are equipped with surgical tools (guides, grippers, a drill, etc.). A specific characteristic of the RONNA system with respect to most current state-of-the-art robotic neurosurgical systems [30-33] is an additional mobile platform equipped with a compliant and

sensitive robotic arm which makes RONNA a dual arm robot system (master and assistant robots). The robots are standard six degree-of-freedom (DOF) revolute robots. This enables full flexibility and reorientations around operative trajectories defined by five parameters (three translations and two rotations).

The system design and functional requirements in neurosurgical robotics are much more demanding than in conventional robotics, e.g. in industrial applications. The robot system has to be compact enough to fit in the OR and should not interfere with the procedure of medical staff. On the other hand, the robot system must meet complex requirements in terms of spatial working ability. Therefore, the robot system setup was designed using CAD software which enabled modelling and simulations [52, 53] of various trajectories and surgical instruments involved in neurosurgery as well as the requirements regarding the location of the whole system in the operating room in relation to other equipment and medical staff.

RONNA is designed to work in a single robot mode or in a dual-arm mode, depending on the type of surgery and the surgeon's choice. In both cases, the patient should be under anaesthesia with the head fixed in a head holder (Mayfield clamp). The master robot is used for the accurate routing of surgical instruments (drill, needle, or any other instrument) to the planned position in the desired orientation. Insertion of the instrument in the direction of the operation point can be done by the assistant robot or by the neurosurgeon. When the operation is performed only with the master robot, the robot is used as a navigation instrument (guide). The extended version of RONNA which uses both robotic arms is intended for automated robotic bone drilling applications and manipulation of surgical instruments. The assistant robot inserts the operating instrument into the tool guide pointing toward the operation point. In addition, the assistant robot is intended for assisting the surgeon through an intuitive human-robot collaboration [54].

The RONNA clinical procedure is composed of three phases: the preoperative phase, the preparation phase, and the operation phase. In the preoperative phase, the bone-attached screws are fixed to the patient's head and the patient is scanned with a CT scanner. After scanning, the patient images are imported into the software for operation planning (RONNAplan) where operation trajectories are planned and the fiducials are localized in the image space. Manual localization of fiducial markers is possible in RONNAplan, but this has shown drawbacks, such as insufficient localization accuracy, long duration, and possibility of human error. To overcome these drawbacks, the automated algorithm for the accurate

localization of spherical fiducials in the image space was developed and is presented as a contribution of this doctoral thesis [55]. The generated surgical plan can automatically be transferred to the robot control software after the planning phase has been completed. Patient registration implies the determination of spatial transformation between the coordinate systems of the medical patient images and the patient in the OR. In the patient registration process, RONNA can use two different marker types (shown in Figure 2.): an x-shaped frame with four standard medical retroreflective spheres (fiducial markers) or freely distributed individual spherical fiducial markers mounted on bone screws.

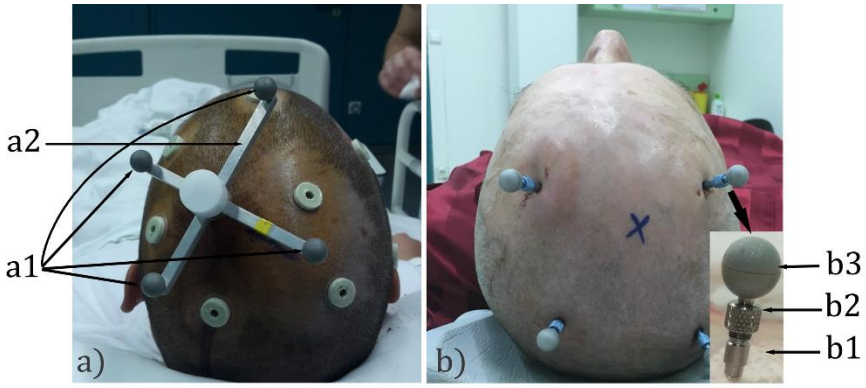


Figure 2. a) The bone-implanted x-shaped frame (a2) with four fiducial markers (a1); b) Freely distributed fiducial markers composed of: (b1) a self-drilling and self-tapping screw, (b2) a removable base, (b3) a retro-reflective sphere, i.e. a fiducial marker

At the start of the surgery, during the preparation phase of the RONNA procedure, the patient is brought to the OR and the robot is positioned near the patient. For the global navigation in the OR, the OTS uses an infrared stereo camera (Polaris Spectra, NDI - Northern Digital Inc., Ontario, Canada) and two reference frames, one attached to the patient and the other to the robotic arm. The OTS is used for coarse positioning of the robot with respect to the patient in the global localization phase of the procedure to enable the automatization of the registration procedure. To solve the rigid point-based registration problem, a correspondence between the physical space and image space fiducials must be established. In the operation phase, the robotic arm is equipped with a stereovision localization device (RONNAstereo) for accurate physical space localization. RONNAstereo consists of two infrared cameras (acA2000-50gmNIR, Basler, Ahrensburg, Germany) with macro lenses aligned at a 55° angle in the same plane. The RONNAstereo has been considerably improved with respect to its initial version presented in [24]. The virtual tool centre point (TCP) of RONNAstereo is calibrated so that it corresponds with the TCP of a calibrated surgical tool. The robot TCP coordinate system is aligned within 0.05 mm using the RONNAstereo TCP and the physical tip of the surgical tool. The stereovision images are processed using a machine vision software running

the circular edge finding algorithm (images shown in Figure 3.) and contrast enchantment that actively determines the position of a localized spherical fiducial with respect to the robot's TCP. The system allows the positioning of the robot's TCP within 0.03mm off a detected spherical fiducial centre.

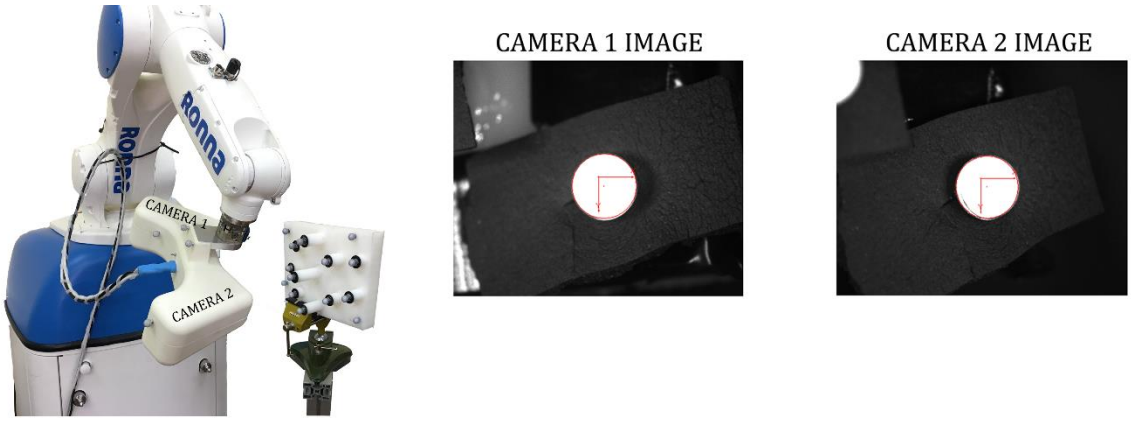


Figure 3. Re-localization of fiducial markers by means of RONNAstereo

Re-localization with RONNAstereo ensures better precision than the sole reliance on the OTS coordinates. After registration, the RONNAstereo is physically replaced with a surgical tool. The surgical tool can then be moved by the robot to any trajectory planned by the surgeon in the preoperative phase.

1.5 Research motivation

In the last two decades, a rapid development of robotic and surgical technologies has taken place. Scientific papers [31], [56], and [57] present an overview, a historical development, and state-of-the-art applications of robotic technology in surgical procedures and in neurosurgery. Robotic challenges in surgical procedures are geometric accuracy and repeatability, safety, programmability of complex 3D paths, automatization of the registration procedure, simple practical usage, and fast adaptation of the system based on multiple sources of sensor data.

Our research group has developed a dual-arm robot system for frameless stereotactic neurosurgery, RONNA. The primary motivation for this doctoral thesis was the opportunity to participate in developing a neurosurgical robot system for clinical application in a rapidly developing scientific field of medical robotics. The research goal is the development of mathematical methods and computer algorithms for spatial registration of the patient in robotic neurosurgery. Spatial patient registration was chosen because it greatly influences primary features of the robot system, such as accuracy, precision, operational setup time,

reliability, safety, flexibility, ease of use; it also enables the development of solutions in the field of computer vision, biomedical image processing, registration, and robot programming. Furthermore, personally, I found high motivation in the opportunity to test the proposed technical and scientific methods and algorithms in the preclinical and the actual clinical environment where the results make a difference in healthcare.

1.6 Objective and hypotheses of the research

The objective of this research is the development of mathematical methods and computer algorithms for spatial registration of the patient in robotic neurosurgery. Since the patient registration includes the patient localization in volumetric images and the physical space, the suggested solution should enable two-way verification of the localized features and estimation of the registration error.

Thesis hypotheses:

1) Automatic fiducial localization in the 3D image space is achievable by estimating the geometrical centre of the fiducial, based on the specific structure forms identified by machine vision algorithms in 2D cross-sections.

2) Localized point correspondence problem and removal of outlier points can be solved by analysing the distance differences of point pairs and error distribution of measuring devices.

1.7 Scientific contribution

The expected scientific contribution of the proposed research:

- an innovative algorithm developed for the recognition of localization features in CT patient images;
- solution to the pair-point correspondence problem in the automatization of the patient registration procedure;
- a model created for the estimation of the robot positioning accuracy based on the registration error.

Scientific contribution of this doctoral thesis is demonstrated in five research papers attached to the thesis and summarized in chapter 6, Conclusion and future work.

2 REGISTRATION

Registration is a general term that describes a process of developing a spatial mapping between two sets of data, or of transforming different sets of data into one coordinate system. In one of the more widely accepted definitions the term *registration implies the aligning of two images of the same environment or object, which can be taken from different viewpoints, with different devices, and at different times* [58]. Due to its fundamental importance, it is used in a number of different research fields including machine vision, robotics, data fusion, object recognition, navigation, and medical imaging. The data used in registration can be point sets in a finite-dimensional real vector space, usually 2D or 3D. If two data sets of points are given, the registration task is to optimally align these two sets of points by estimating the best transformation between them. Real data include measurement and localization errors which reduce the alignment accuracy in the registration process. Besides the aforementioned problems regarding errors that prevent optimal localization, the correspondences between points in the sets are often not known apriori, which makes the registration problem challenging. In that case, the registration problem is also known as the simultaneous pose and correspondence problem (SPC) [59]. Given the nature of the registration, we can differentiate between the rigid and the non-rigid registration. The term rigid transformation has been derived from the definition of a rigid body: *A rigid body is a collection of particles moving in such a way that the relative distances between the particles do not change* [60]. Hence, a rigid transformation is defined as a transformation that does not change the distance between any two points; typically, such a transformation consists of translation and rotation. A rigid body transformation in 3D is defined by six parameters, three translations and three rotations [61]. On the other hand, non-rigid registration can yield elastic transformation between the two point sets. Non-rigid transformations, such as scaling and shear mapping, typically involve nonlinear transformations. In neurosurgical procedures, the skull can be classified as a rigid body and hence, in this research, the focus is on the rigid registration.

2.1 Mathematical background

The mathematical background chapter in this thesis is based on the text and mathematical expressions found in [60, 62]. Consider a rigid body with $N + 1 > 3$ number of

points, denoted as $\mathbf{p}_0, \ldots, \mathbf{p}_N$, with known relative distances. To determine the number of parameters that are needed to specify the position of all the points we could use $3(N + 1)$ coordinates of the points, but the rigid body constraint can reduce the necessary number of parameters. Three parameters are needed to define the spatial position of point $\mathbf{p}_0$. Another point, $\mathbf{p}_1$, can be located with two additional parameters relative to the first point. The third point, $\mathbf{p}_2$, is at a fixed distance from the first two points. Once the position of three points is fixed, the positions of the remaining $N - 2$ points are also fixed. This means that six parameters will determine the coordinates of every point in the body. The rigid body transformation can be composed of translations of the reference point $\mathbf{p}_0$ and the rotation about that reference point.

The translation $\mathbf{T_a}$ moves each point $\mathbf{p}$ to $\mathbf{p}$+$\mathbf{a}$. By applying the transformation $\mathbf{T}_{\mathbf{p'}_0 - \mathbf{p}_0}$ to each point on a rigid body

$$\mathbf{p}_i \longrightarrow \mathbf{p'}_i, \qquad i = 0, \ldots, N, \tag{1}$$

intermediate positions denoted as $\tilde{\mathbf{p}}_0$ and $\tilde{\mathbf{p}}_i$ are produced:

$$\tilde{\mathbf{p}}_0 = \mathbf{p'}_0 \text{ and } \tilde{\mathbf{p}}_i = \mathbf{T}_{\mathbf{p'}_0 - \mathbf{p}_0}(\mathbf{p}_i) = \mathbf{p}_i + (\mathbf{p'}_0 - \mathbf{p}_0), \qquad i = 0, \ldots, N. \tag{2}$$

If the transformation fixes $\mathbf{p'}_0$ and moves each $\tilde{\mathbf{p}}_i$ to $\mathbf{p'}_i$, we get a rigid body transformation with a fixed point, i.e. a rotation. A rotation is a linear transformation that fixes the origin point and preserves the lengths of vectors and the orientation of bases. If rotation is denoted with $\mathbf{R}$, the action on $\mathbf{p}_i$ is:

$$\mathbf{p'}_i = \mathbf{p}_0 + (\mathbf{p'}_0 - \mathbf{p}_0) + \mathbf{R}(\tilde{\mathbf{p}}_i - \mathbf{p'}_0) = \mathbf{p}_0 + \mathbf{a} + (\mathbf{p}_i - \mathbf{p}_0), \quad \mathbf{a} = \mathbf{p'}_0 - \mathbf{p}_0 \tag{3}$$

If we take $\mathbf{p}_0 = 0$, then the rigid body transformation can be written as:

$$\mathbf{p'} = \mathbf{Rp} + \mathbf{a} \tag{4}$$

If this action is followed by another rigid body transformation,

$$\mathbf{p''} = \mathbf{Qp'} + \mathbf{b} \tag{5}$$

$$\mathbf{p''} = \mathbf{QRp} + \mathbf{Qa} + \mathbf{b} \tag{6}$$

In that case, the new rigid body transformation has the rotation $\boldsymbol{T} = \boldsymbol{QR}$ and the translation $\mathbf{c} = \mathbf{Qa} + \mathbf{b}$. The inverse of $\mathbf{p'}$is equal to

$$\mathbf{R}^{-1}\mathbf{p}' - \mathbf{R}^{-1}\mathbf{a} = \mathbf{p} \tag{7}$$

Rigid body transformations form a special Euclidean group, SE(3), which consists of pairs (**R**,**b**), where **R** is the rotation and **b** the vector, with a binary operation ∘,

$$(\mathbf{R}, \mathbf{a}) \circ (\mathbf{Q}, \mathbf{b}) = (\mathbf{RQ}, \mathbf{Rb} + \mathbf{a}) \tag{8}$$

The inverse is equal to:

$$(\mathbf{R}, \mathbf{a})^{-1} = (\mathbf{R}^{-1}, -\mathbf{R}^{-1}\mathbf{a}) \tag{9}$$

If we have a vector **p** such that

$$\mathbf{p} = \begin{pmatrix} \mathbf{p}_1 \\ \mathbf{p}_2 \\ \mathbf{p}_3 \end{pmatrix} \tag{10}$$

points of $\mathbb{R}^3$ may be represented in homogeneous coordinates as $\begin{pmatrix} \boldsymbol{p} \\ 1 \end{pmatrix}$, in which case the rigid body transformation $(\mathbf{R}, \mathbf{a})$ is represented by the 4x4 matrix written as

$$\begin{pmatrix} \mathbf{R} & \mathbf{a} \\ 0 & 1 \end{pmatrix} \tag{11}$$

and

$$\begin{pmatrix} \mathbf{R} & \mathbf{a} \\ 0 & 1 \end{pmatrix} \begin{pmatrix} \mathbf{p} \\ 1 \end{pmatrix} = \begin{pmatrix} \mathbf{Rp} + \mathbf{a} \\ 1 \end{pmatrix} \tag{12}$$

When registering two data sets in the 3D space it is necessary to estimate six parameters that best describe the transformation matrix. If the transformation matrix **M** is shown in a form

$$\mathbf{M} = \mathbf{T_a R}, \tag{13}$$

where

$$\mathbf{T_a} = \begin{bmatrix} 1 & 0 & 0 & q_1 \\ 0 & 1 & 0 & q_2 \\ 0 & 0 & 1 & q_3 \\ 0 & 0 & 0 & 1 \end{bmatrix} \tag{14}$$

and

$$\mathbf{R} = \begin{bmatrix} 1 & 0 & 0 & 0 \\ 0 & \cos(q_4) & \sin(q_4) & 0 \\ 0 & -\sin(q_4) & \cos(q_4) & 0 \\ 0 & 0 & 0 & 1 \end{bmatrix} \begin{bmatrix} \cos(q_5) & 0 & \sin(q_5) & 0 \\ 0 & 1 & 0 & 0 \\ -\sin(q_5) & 0 & \cos(q_5) & 0 \\ 0 & 0 & 0 & 1 \end{bmatrix} \begin{bmatrix} \cos(q_6) & \sin(q_6) & 0 & 0 \\ -\sin(q_6) & \cos(q_6) & 0 & 0 \\ 0 & 0 & 1 & 0 \\ 0 & 0 & 0 & 1 \end{bmatrix} \tag{15}$$

it is necessary to stress that the matrix multiplication is not commutative; therefore, the order of matrices matters. If s_4, s_5, and s_6 are the sines, and c_4, c_5, and c_6 are the cosines of parameters q_4, q_5, and q_6, respectively, then we can show the rotation matrix as:

$$\mathbf{R} = \begin{bmatrix} c_5c_6 & c_5s_6 & s_5 & 0 \\ -s_4s_5c_6 - c_4s_6 & -s_4s_5s_6 + c_4c_6 & s_4c_5 & 0 \\ -c_4s_5c_6 + s_4s_6 & -c_4s_5s_6 - s_4c_6 & c_4c_5 & 0 \\ 0 & 0 & 0 & 1 \end{bmatrix} \tag{16}$$

If c_5 is not zero, then parameters q_4, q_5 and q_6 are:

$$q_5 = \sin^{-1}(r_{13}) \tag{17}$$

$$q_4 = \text{atan2}(r_{23}/\cos(q_5), r_{33}/\cos(q_5)) \tag{18}$$

$$q_6 = \text{atan2}(r_{13}/\cos(q_5), r_{11}/\cos(q_5)) \tag{19}$$

where atan2 is the four-quadrant inverse tangent.

2.2 Registration methods and algorithms

Registration algorithms used for the geometric alignment of 3D point data are a well-researched topic in the fields of robotics and computer vision. Bellekens et al. [63] give an overview of the state-of-the-art registration methods, such as Singular Value Decomposition (SVD), Principal Component Analysis (PCA), and Iterative Closest Point (ICP) algorithm [64] with its variants. These methods are mostly used for processing the data collected from various 3D sensors. Any device that generates spatial input data generates positioning errors as a consequence of environmental signal noise, errors produced due to the discretization of the input signal, and the resolution of the device itself. This means that there is a great possibility that due to the errors in data there will be incorrect correspondences between the input points, as shown in Figures 5. and 6. The incorrect correspondences are called outliers and if they are not removed, they will impair the accuracy of the estimated transformation.

The SVD method uses the cross-correlation matrix to calculate the optimal transformation (in the least squares sense) between two point clouds when the exact correspondence between point pairs is known. The translation and rotation accomplished by SVD are shown in Figure 4., while a solution for acquiring the transformation matrix using the SVD method is given in section 2.4 dealing with SVD.

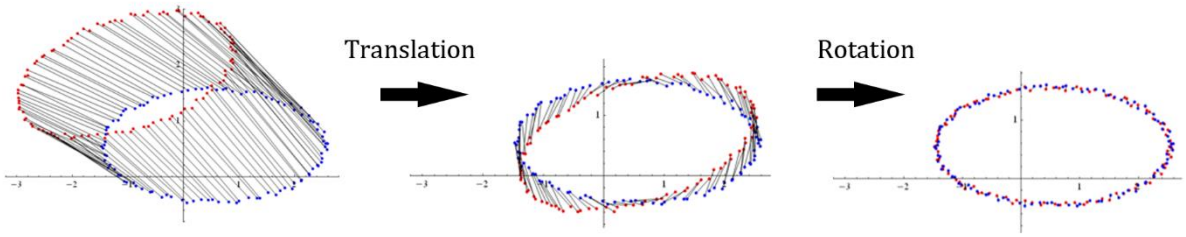


Figure 4. The SVD method results for known correspondence between point pairs [64]

The principal component analysis (PCA) gives a rotation matrix when aligning the directions of the largest eigenvectors extracted from the covariance matrices of the two datasets. Since the PCA method is very sensitive to outlier points, it is generally used only as the first rough estimation of the initial transformation in other algorithms such as the iterative closest point (ICP). Outliers shown in the blue set of points in Figure 5. are mainly responsible for the impaired transformation between the two sets.

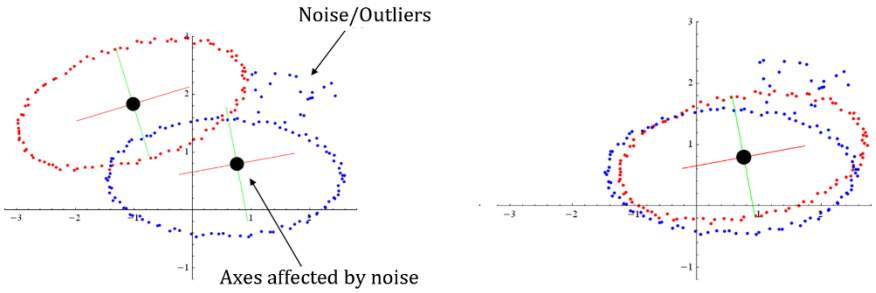


Figure 5. An example of the principal component analysis (PCA) [64]

The ICP algorithm guesses the point correspondences between the data sets based on the nearest neighbour approach and iteratively refines the transformation. After each iteration, the outliers are disregarded in order to improve the previous estimate of the transformation parameters.

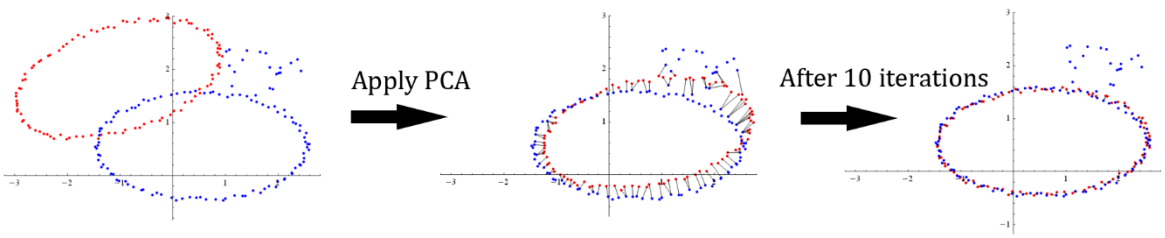


Figure 6. An example of the iterative closest point (ICP) method[64]

Since ICP is an iterative local minimization method, it is sensitive to the initial alignment of the data.

2.3 Correspondence problem

The correspondence problem is a fundamental task which is found in applications such as image and point cloud alignment, optic flow estimation, 3D reconstruction, and stereo vision [65, 66]. If we consider that every scene can be viewed from different viewpoints, or with different equipment (stereovision cameras, range lasers, 2D cameras, medical scanners, etc.), then the problem is in connecting the resulting points or pixels. The solution to the correspondence problem is finding correct point-to-point or pixel-to-pixel correspondences between models or images. The purpose of finding the correspondences is to eventually determine the displacement field vector, i.e. in a 3D case, the 4x4 transformation matrix. The correspondence problem is made more difficult due to the errors in data that can cause incorrect correspondences between the input points. If outliers are not removed, they will impair the accuracy of the estimated transformation. As elaborated in the paper [67], current 3D correspondence techniques are much less accurate than those of their 2D counterparts because of a higher rate of outliers.

In comparison with most of the recent research in the field of registration and point-pair correspondence, our problem in this doctoral thesis (extrinsic marker registration in robotic neurosurgery) is very specific because we are dealing with small data sets containing up to ten points; in addition, the sets contain noise from the input devices and possibly outlier points. Sets of up to ten points are realistic in regard to the number of fiducial markers used in standard neurosurgical applications. Since we register data sets in a medical environment, the solution to our particular correspondence problem has to ensure greater safety. It is of paramount importance for the algorithm to get the correct correspondence between every point pair in the presence of noise and potential outlier points and to determine with a high level of statistical confidence that the mathematical solution is unique. Furthermore, it is important that no actual fiducial markers are classified as outliers. From the perspective of computing speed, the extenuating circumstance is that the number of used fiducial markers is always relatively small.

To solve our specific problem, we have developed a novel correspondence algorithm that is presented in [68]. Once the algorithm finds the correspondence between two points to form a

pair, we can implement the closed-form SVD method for finding the rigid transformation that optimally aligns two sets of fiducial marker coordinates in the least squares sense.

2.4 Singular Value Decomposition (SVD)

The implementation of the SVD is based on the technical notes entitled *Using SVD for some fitting problems* [69] and *Least squares rigid motion using SVD* [70]. For the case of a matrix $\in \mathbb{R}^{m\times n}$, the singular value decomposition is:

$$\mathbf{A} = \mathbf{USV}^{\mathrm{T}}, \tag{20}$$

where:

$\mathbf{U} \in \mathbb{R}^{m\times m}$ is the first orthogonal matrix;

$\mathbf{V} \in \mathbb{R}^{n\times n}$ is the other orthogonal matrix;

$\mathbf{S} \in \mathbb{R}^{m\times n}$, is a diagonal matrix with singular values on the main diagonal → $\sigma_1 \geq \sigma_2 \geq \cdots, \geq \sigma_{\mathrm{r}} \geq 0, \mathrm{r} = \min(m, n)$.

For two sets of corresponding *n* number of 3D points $\{\mathbf{x}_1 \ldots \mathbf{x}_{\mathrm{n}}\}$ and $\{\mathbf{y}_1 \ldots \mathbf{y}_{\mathrm{n}}\}$, the rotation matrix **R** and the translation vector **t** are calculated by mapping the first set of points to the second. Transformation is not exact due to the measurement errors, so the least square problem is as follows:

$$\min_{\mathbf{R}\in\Omega,\mathbf{t}} \sum_{\mathrm{i}=1}^{\mathrm{n}} \|\mathbf{R}\mathbf{x}_{\mathrm{i}} + \mathbf{t} - \mathbf{y}_{\mathrm{i}}\|^2, \tag{21}$$

where $\Omega = \{\mathbf{R} \mid \mathbf{R}^{\mathrm{T}}\mathbf{R} = \mathbf{R}\mathbf{R}^{\mathrm{T}} = \mathrm{I}_3; \det(\mathbf{R}) = 1\}$ is the set of orthogonal rotation matrices. Here, **A** and **B** are introduced:

$$\mathbf{A} = [\mathbf{x}_1 - \bar{\mathbf{x}}, \ldots, \mathbf{x}_{\mathrm{n}} - \bar{\mathbf{x}}] \tag{22}$$

$$\mathbf{B} = [\mathbf{y}_1 - \bar{\mathbf{y}}, \ldots, \mathbf{y}_{\mathrm{n}} - \bar{\mathbf{y}}] \tag{23}$$

where :

$$\bar{\mathbf{x}} = \frac{1}{n}\sum_{i=1}^{n} \mathbf{x}_{\mathrm{i}} \tag{24}$$

$$\bar{\mathbf{y}} = \frac{1}{n}\sum_{i=1}^{n} \mathbf{y}_{\mathrm{i}} \tag{25}$$

With A and B, the non-linear problem of determining the rotation matrix is expressed as:

$$\min_{\mathbf{R}\in\Omega}\|\mathbf{RA}-\mathbf{B}\|_{\mathrm{F}}, \tag{26}$$

with the Frobenius norm of a matrix $\mathbf{Z}$ defined as:

$$\|\mathbf{Z}\|_{\mathrm{F}}^{2}=\sum_{\mathrm{i,j}}\mathbf{z}_{\mathrm{i,j}}^{2} \tag{27}$$

Finally, the problem can be solved as a singular value decomposition of the matrix:

$$\mathbf{C}=\mathbf{BA}^{\mathrm{T}} \tag{28}$$

Where

$$\mathbf{USV}^{\mathrm{T}}=\mathbf{C} \tag{29}$$

Rotation is then expressed as:

$$\mathbf{R}=\mathbf{U}\,\mathrm{diag}(1,1,\det(\mathbf{UV}^{\mathrm{T}}))\mathbf{V}^{\mathrm{T}} \tag{30}$$

and translation as:

$$\mathbf{t}=\bar{\mathbf{y}}-\mathbf{R}\bar{\mathbf{x}} \tag{31}$$

3 PATIENT LOCALIZATION

In medical robotics, patient localization is defined as the process of determining the exact position or coordinates of the patient in the image space or the physical space. The patient in the image space is given as 3D data acquired by using preoperative medical scans. The patient in the physical space is defined by its 3D position in the OR in the coordinate system of a localization device. Finding point pairs between two sets of points, $\{\mathbf{x}_i\}$ and $\{\mathbf{y}_i\}$, which after transformation have the root-mean-square (RMS) distance between the points equal to zero, would mean that both inputs have zero positioning errors and no outlier points. In actual situations, the positioning errors from input devices are a consequence of environmental signal noise, errors produced due to the discretization of the input signal, and the resolution of the device itself. Errors which occur in the localization procedure reduce the alignment accuracy and have a negative effect on the registration accuracy. The positions of the individual points that are localized with an error, can be written as shown in [71]:

$$\mathbf{x}_i = \hat{\mathbf{x}}_i + \mathbf{e}_{\mathbf{xi}} \tag{32}$$

$$\mathbf{y}_j = \hat{\mathbf{y}}_j + \mathbf{e}_{\mathbf{yj}}, \tag{33}$$

where $\hat{\mathbf{x}}_i$ and $\hat{\mathbf{y}}_j$ are the true point coordinates and $\mathbf{x}_i$ and $\mathbf{y}_j$ are respectively the coordinates from the patient images and the patient in the OR, which contain their errors $\mathbf{e}_{\mathbf{xi}}$ and $\mathbf{e}_{\mathbf{yj}}$.

3.1 Image space localization

Localization of the patient in the image space is the determination of the position of reference points in the coordinate system of the medical scanning device. In neurosurgical procedures, CT, MR or other imaging technologies are usually used prior to surgery for patient scanning, diagnosis and surgery planning. Three primary imaging planes used are: axial plane (transverse), sagittal plane (lateral view that separates the left and the right sides of the body) and coronal plane (frontal view which separates the front from the back). A number of images or slices are acquired in one 2D plane and then used to reconstruct images in other planes or the 3D model. Figure 7. shows a series of axial CT head slices. Reference points for the “image space-to-physical space” registration process can also be called fiducial points. For the registration to be successful at least three corresponding fiducial points need to be localized in the coordinate system of the medical scanning device and later in the OR.

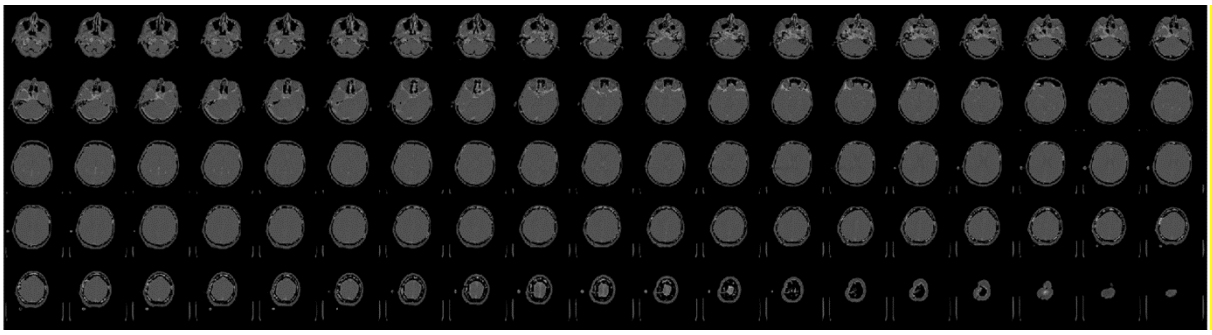


Figure 7. Series of axial CT head slices

Errors which occur in the localization procedure reduce the alignment accuracy in the registration process and have a negative effect on the registration accuracy. Patient localization can be based on different types of references. Registration and localization methods with regard to the type of reference used are extrinsic, intrinsic, and non-image based (calibrated coordinate systems) [72]. Extrinsic methods rely on attaching external objects to a patient prior to imaging, while intrinsic methods use the patient's anatomical landmarks [73]. External objects used in medical procedures are stereotactic frames, rigid bone-attached markers, other externally attached frames, and adhesive markers. Advantages of extrinsic methods in terms of accuracy in comparison with the intrinsic and calibration-based methods are identified and evaluated in [4]. In the study, seven different modes of patient registrations were compared based on in vivo measurements including thirty patients. Bone-attached markers provided the highest degree of the application and the targeting accuracy when used in IGIs.

3.2 Physical space localization

Localization in the physical space is the process of determining the exact patient coordinates in the coordinate system of the localization (measuring) device located in the operating room. There are many different sensor technologies that can be used for physical space localization. Most commonly used devices are vision sensors (mono-camera, stereo-camera, optical tracking system - OTS), touch sensors (force-torque) and magnetic sensors. The main two approaches in the robot localization are:

- localization device is independent of the robot and acquires the position of both the robot and the patient simultaneously,
- the sensor itself is mounted on the robotic arm.

In the RONNA system we use both approaches, OTS for global localization, and RONNAstereo mounted on the robotic arm for precise patient localization. If the sensor is

mounted on the robot, its performance in regards to positioning ability becomes an important factor. Robot repeatability is defined as the ability of the robot to return to the same position and orientation. In medical robotics absolute accuracy is a more significant factor than repeatability since the robot is sent to arbitrary target positions and orientations. Robot absolute accuracy is defined as the ability of a robot to move to the desired position in three-dimensional (3D) space with respect to a reference frame [74, 75]. Robot accuracy can also be defined as the difference between the calculated and the resulting robot position. In comparison to repeatability, accuracy error is usually an order of magnitude larger [76]. The robot positioning error is a result of the difference between the ideal kinematic model of the robot and the actual unit. Factors that cause robot errors are manufacturing and assembly imperfections, influence of temperature on the dimensions and material characteristics of a robot part, backlash and resolution of encoders [77]. Robot accuracy can be improved by using calibration methods. Research in the field of robot calibration focuses on various types of model optimization [78-80] and on the development of measuring equipment and techniques used for calibration [81, 82]. Since the equipment for robot calibration can be expensive and the calibration procedure is a time-consuming task, in this doctoral thesis we have demonstrated that the application error of the robot system can also be reduced without the use of calibration methods as a good choice of robot localization strategy can ensure that.

Regarding the types of markers used in robotic neurosurgery, non-invasive markers are preferred because of a simpler mounting procedure, on the other hand they show lower accuracy and hence their usage is limited to procedures which do not require the highest level of accuracy. For example, the stereotactic robot system ROSA is used in intracranial procedures [83]. In [17], Lefranc et al. assess the impact of imaging modality, registration method, and intraoperative flat-panel computed tomography on the application accuracy of the ROSA stereotactic robot. Their measurements show that the frame-based stereotactic registration in robotic surgery is more accurate than the frameless (markerless) registration. In vitro testing of the Neuromate neurosurgical robot showed similar results regarding the impact of the selected registration method on the application accuracy. In vitro testing [84] showed that the application accuracy of the frame-based localization system was 0.86 ± 0.32 mm and that of the frameless localization system 1.95 ± 0.44 mm. In a more recent study [85], in vitro and in vivo tests carried out with the Neuromate's frame-based application showed even more improved accuracy.

4 ERROR ANALYSIS

The definition of positioning accuracy of a neurosurgical robot is the distance between the planned targets defined in the image space by the surgeon and the actual positions reached with the surgical instrument attached to the robot. Neurosurgical robot accuracy can be explained through three different aspects: robot intrinsic accuracy, registration accuracy, and application accuracy. The most relevant factor for the surgeons and the patients is the overall positioning accuracy, i.e. the application accuracy. Major factors influencing the registration accuracy are the fiducial marker type, the number of used fiducial markers, the spatial distribution of fiducial points and the accuracy of the localization method. In the study [86], the idea of improving the target registration accuracy is proposed through the optimization of the distribution of fiducial points when the planned target trajectory is known. The study provides a practical approach for the surgeon to arrange the fiducial markers in a way that reduces the target registration error. A similar research also presents different approaches and performance metrics that can be used when planning the placement of fiducial markers [87, 88]. Fitzpatrick et al. [89] show that a greater spread of fiducials leads to greater registration accuracy. Concerning the number of fiducial markers, Perwög et al. [90], show in their study that the larger number of fiducial markers used in the registration had a positive influence on the accuracy of the computer-assisted navigation. This is one of the factors of the robot system that was tested in this thesis.

4.1 Measures of localization and registration errors

The transformation that maps the rigid body points between the image space and the physical space in real applications is considered to be imperfect and should contain certain errors. To evaluate the registration performance, three types of error have been studied in the theory of the medical image registration error introduced by Fitzpatrick et al. [91, 92]: fiducial registration error, fiducial localization error, and target registration error. Fiducial registration error (FRE) is an error in aligning the corresponding fiducials after registration. FRE is defined as the root mean square distance between two sets of n matching fiducials after registration:

$$FRE^2 = \frac{\sum_{j=1}^{n} \|\mathbf{q}_j - \mathbf{M}(\mathbf{p}_j)\|^2}{n}, \tag{35}$$

with $\mathbf{q}_j$ being the position of a single fiducial in the image space, and $\mathbf{p}_j$ being the exact position of a fiducial in the physical space. **M** is the rigid body transformation between the two sets. Fiducial localization error (FLE) is defined as the Euclidean distance between the true and the measured distance of the fiducial location. According to the aforementioned theory and a more recent study [93], if the ground truth measurement is available, FLE can be estimated based on the *n* number of fiducials and the FRE as:

$$FLE_{\mathrm{GT}}^2 = \frac{n}{n-2} FRE^2 \tag{36}$$

Intra-modal FLE estimation is based on two or more different CT scans of the same set of fiducials; it can be calculated as:

$$FLE_{\mathrm{IMAGE}}^2 = \frac{1}{2}\frac{n}{n-2} FRE^2, \tag{37}$$

for two different CT scans, or as:

$$FLE_{\mathrm{IMAGE}}^2 = \frac{n}{2M(n-2)} \sum_{m=1}^{M} FRE_m^2, \tag{38}$$

for more than two scans. *M* is the number of different registrations and FRE_m is the FRE of the *m*-th registration. In clinical application, the positioning accuracy of the targeted points is the most significant element. Target registration error (TRE) is defined as the distance between the planned image target location and the physical target location after registration. TRE can be estimated as the error in a given position **p** that may be caused by FLE. Assuming an isotropic error distribution of FLE, the norm of TRE can be estimated as in [92, 94]:

$$TRE^2(\mathbf{p}) \approx \frac{FLE^2}{n}\left(1 + \frac{\sum_{k=1}^{3}\frac{d_k^2}{f_k^2}}{3}\right), \tag{39}$$

with *n* being the number of fiducials, d_k the minimal distance of **p** from the *k*-th principal axis, and f_k the RMS distance of the fiducials from the *k*-th axis. It should be noted that even though equations (36-38) and (39) are found to be a reliable estimate of FLE and TRE, there are cases in which FRE does not approach the FLE as the number of fiducials increases and the TRE from (39) is uncorrelated with the true TRE [95]. In [96] it is shown that for a single clinical case FRE and TRE are uncorrelated but equations (36-38) can be used to estimate the mean value of FLE from FRE based on many measurements. The target registration error can be estimated from the fiducial localization error for that specific fiducial configuration and target position.

4.2 Error analysis of a neurosurgical robot system

Positioning errors of a neurosurgical robot system are manifested in the physical space. Robot intrinsic accuracy and registration accuracy are the two major factors which generate the application accuracy of a neurosurgical robot system. Liu et al. [97] analysed and improved the application accuracy of Neuromaster, a 5 degree-of-freedom (DOF) neurosurgical robot system. In their research, the focus was on the improvement of the intrinsic accuracy of the robot through the use of neural networks for the compensation of joint transmitting error. The analysis of the robot positioning error in that research applies to ours.

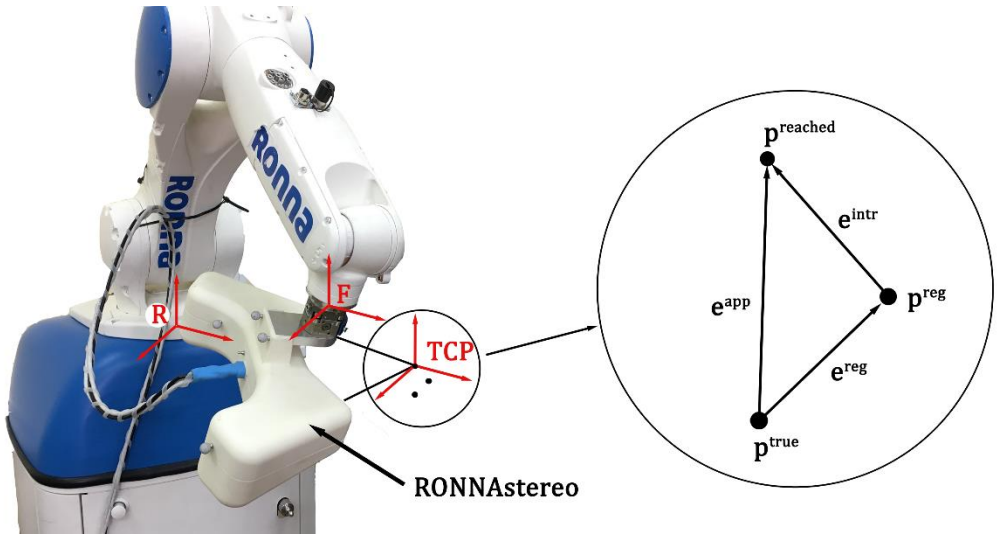


Figure 8. Demonstration of the neurosurgical robot system positioning errors

Application error of the robot system $\mathbf{e}^{\text{app}}$, regardless of the reference coordinate system, is the distance between the true position of the target $\mathbf{p}^{\text{true}}$ and the actual position the robot tool has reached $\mathbf{p}^{\text{reached}}$. In our research, two infrared cameras with macro lenses (RONNAstereo) attached to the robot flange as shown in Figure 8., are used for the localization of fiducial markers and measuring of the application error. The magnitude of the robot system application error is given as a sum of the registration error $\mathbf{e}^{\text{reg}}$ and the robot intrinsic error $\mathbf{e}^{\text{intr}}$:

$$\|\mathbf{e}^{\text{app}}\| = \|\mathbf{e}^{\text{reg}} + \mathbf{e}^{\text{intr}}\| \tag{40}$$

The point $\mathbf{p}^{\text{reg}}$ is the point which is transformed from the image space to the physical space in the registration procedure; it can be defined as:

$$\mathbf{p}^{\text{reg}} = \mathbf{p}^{\text{true}} + \mathbf{e}^{\text{reg}}, \tag{41}$$

where $\mathbf{e}^{\mathrm{reg}}$ is the target registration error (TRE), the distance between the planned image target location and the physical target location after the registration. The magnitude of TRE or $\mathbf{e}^{\mathrm{reg}}$ depends on the number of fiducial markers, the spatial configuration of fiducial markers, the location of target points and the localization error. FLE is present in both the image and the physical space. FLE in the image space is a result of noise produced by imaging artefacts, the resolution of the reconstructed images produced by the CT or the MRI scanner, and the accuracy of the localization method. For our robot system, FLE in the physical space is a consequence of robot positioning errors during localization, calibration between the robot flange and RONNAstereo, resolution of the two cameras, and the algorithm used for calculating the centres of fiducial markers. In their study, Siebold et al. [98], use TRE for the approximation of the safety margin between the drill tip and the nearby anatomical structures during the robotic bone milling task. The difference between the point where the robot is sent to, $\mathbf{p}^{\mathrm{reg}}$, and the point that the tool tip reaches, $\mathbf{p}^{\mathrm{reached}}$, is the robot intrinsic error $\mathbf{e}^{\mathrm{intr}}$:

$$\mathbf{p}^{\mathrm{reached}} = \mathbf{p}^{\mathrm{reg}} + \mathbf{e}^{\mathrm{intr}} \tag{42}$$

The position of the robot is defined by six joint angles $\boldsymbol{\theta} = (\theta_1, \theta_2, \theta_3, \theta_4, \theta_5, \theta_6,)$, while a change in the robot tool position is determined by the change of the robot joint angles. The position of the robot tool (TCP) in the Cartesian coordinate system can be calculated based on the robot kinematic model in the coordinate system of the robot base **R** as:

$$\mathbf{R}_{\mathbf{TCP}}\mathbf{A} = {}^{\mathbf{R}}_{1}\mathbf{A} \cdot {}^{1}_{2}\mathbf{A} \cdot {}^{2}_{3}\mathbf{A} \cdot {}^{3}_{4}\mathbf{A} \cdot {}^{4}_{5}\mathbf{A} \cdot {}^{5}_{\mathbf{F}}\mathbf{A} \cdot {}_{\mathbf{TCP}}^{\mathbf{F}}\mathbf{A}\,, \tag{43}$$

where each homogenous transformation matrix ${}^{\mathrm{i}-1}_{\mathrm{i}}\mathbf{A}$ is a function of the i-th joint variable $\boldsymbol{\theta}$ and the physical size of the associated link.

Concerning the differences between the robot kinematic model and the physical unit, it is expected that greater changes in robot joint angles or greater distances between points should typically result in a larger deviation of the real robot tool position from the position calculated based on its nominal kinematic model. From the perspective of the neurosurgical robot positioning accuracy, this means that if the target is further away from the fiducial markers or if the orientation of the trajectory differs from the orientation of the robot during the localization of fiducial markers, then we could expect larger positioning errors.

5 SELECTED RESULTS AND DISCUSSION

In this chapter, the research results from the published papers are extracted and discussed as the thesis contributions. Papers which are a part of this doctoral thesis are referenced in the literature and named with uppercase letters and a number according to their order of appearance in the section Summary of papers and the section Appendix.

5.1 Automated localization in the image space

Major challenges associated with extrinsic automated localization in the image space are:

- detection of features associated with fiducial markers,
- autonomous detection and removal of false positives (features which are not part of the fiducial markers) in the cluttered image space environment,
- accurate approximation of centre of fiducial markers (fiducial points) based on the detected features of fiducial markers,
- shortening the processing time.

The main motivation for the development of the image space localization algorithm was to enable full autonomy, to improve the main features of image space localization (accuracy, robustness to noise and speed of execution) and to replace the previous localization method i.e. manual localization done by the surgeon. The main disadvantages of manual localization are localization duration, possible human error, and insufficient accuracy. In the RONNA neurosurgery procedure, manual localization must be conducted after the patient with the attached fiducial marker has been scanned and taken to the operating room. The surgeon then visually determines the centre of every spherical fiducial in the exact order as that in which the coordinate system has been defined. Since the neurosurgeon can only start with the target planning after the localization procedure, it is crucial that this phase takes as little time as possible. Obviously, this increases the pressure on the surgeon.

In PAPER 1 [55], the algorithm for automatic localization of spherical fiducials in CT scans is presented and clinically evaluated. In that paper, we presented a novel algorithm for the accurate localization of fiducial markers in the image space (CT scans). The drawbacks of

manual localization are overcome by means of biomedical image filtrations, machine vision algorithms and mathematical approximation methods. An extrinsic, bone-implanted x-shaped frame with four retro-reflective spherical fiducials is used for localization. The pre-processing step in the automatic localization algorithm includes an intensity-based filtration of voxels, thus, the slices where fiducial markers are located are segmented as regions of interest (ROI). In some cases, false positive results, i.e. false positive ROIs, are identified in the area of the patient's teeth because of dental fillings. After that step, the Circular Hough Transform (CHT)-based algorithm is used for finding all the potential circles in two orthogonal image projections (axial and sagittal). Due to the visually cluttered environment in 2D CT images, many false positive circles are detected. An iterative clustering method was developed for circle grouping. Verified clusters are used for calculating the fiducial markers centres. Euclidean distance filters are used for clustering and for elimination of potential false positive results. Two methods for estimating spherical fiducial centres from the detected clusters are implemented: RANSAC Linefit and Spherefit. More details on the development and the scientific contribution of the localization algorithm are available in the published paper.

Robustness, accuracy, reliability, and processing time of the algorithm for the automated localization of fiducial markers were verified in the conducted clinical trials. The performance of the localization algorithm was evaluated in comparison with four skilled human operators. The measurements were based on twelve patient and eight lab phantom CT scans. The localization error of the algorithm in comparison with the human readings was smaller by 49.29% according to the ground truth estimation (Table 2) and by 45.91% according to the intra-modal estimation (Table 3).

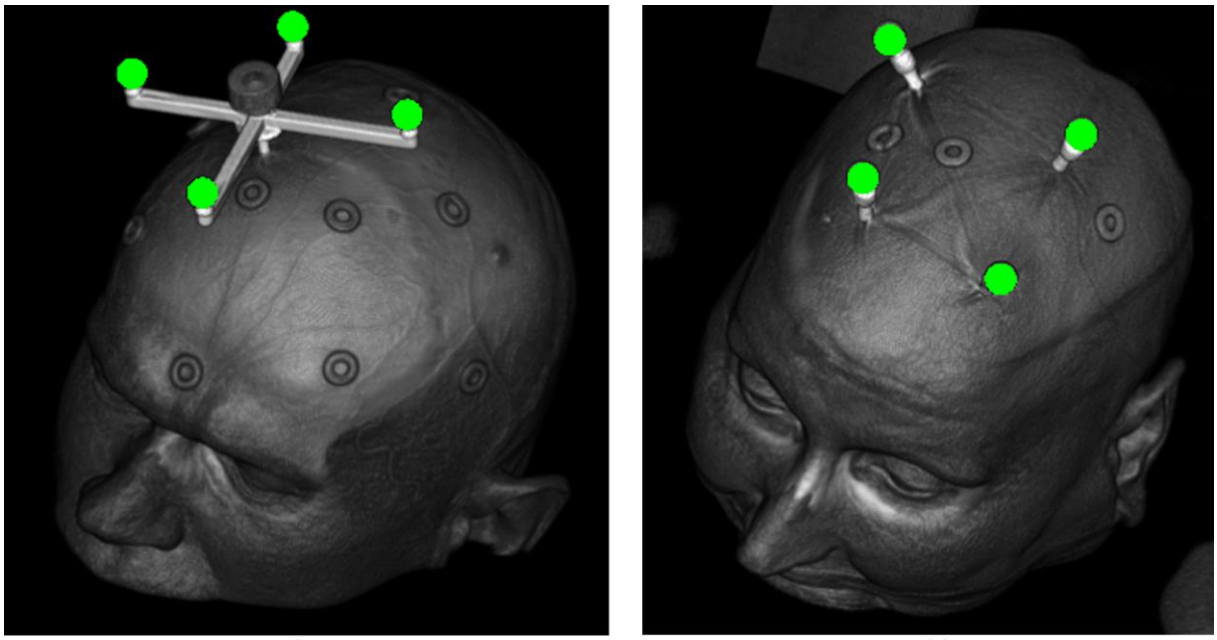
Table 2. Ground truth estimation of phantom fiducial localization error (FLE)

	FLE_{GT}		
Image set number	**Human operators**	**Algorithm Linefit**	**Algorithm Spherefit**
1	0.2956	0.0986	0.1030
2	0.3043	0.1627	0.0799
3	0.2243	0.0678	0.1042
4	0.3558	0.2354	0.2307
5	0.4146	0.2780	0.2907
MEAN FLE_{GT}	**0.3189**	**0.1685**	**0.1617**

Table 3. Intra-modal estimation of phantom fiducial localization error (FLE)

Registration number	FRE						
	Human operator 1	**Human operator 2**	**Human operator 3**	**Human operator 4**	**Avg.human operator**	**Algorithm Linefit**	**Algorithm Spherefit**
1	0.3471	0.2454	0.3123	0.4643	0.3605	0.1748	0.1218
2	0.5055	0.3918	0.4241	0.8468	0.4075	0.0638	0.0731
3	0.504	0.1204	0.3983	0.6072	0.4047	0.2018	0.2125
4	0.413	0.1664	0.3678	0.7419	0.4021	0.2857	0.2785
5	0.7072	0.6116	0.5293	0.761	0.4222	0.1327	0.1300
6	0.5486	0.2623	0.3361	0.4719	0.4165	0.3568	0.2506
7	0.3625	0.2946	0.2779	0.7309	0.5543	0.1466	0.2508
8	0.3085	0.3788	0.3843	0.5366	0.3423	0.2458	0.1798
9	0.459	0.3697	0.3205	1.0682	0.5421	0.2470	0.3310
10	0.2483	0.1653	0.2648	0.7636	0.6523	0.4830	0.4673
MEAN FRE	**0.4403**	**0.3006**	**0.3615**	**0.6992**	**0.4504**	**0.2338**	**0.2295**
FLE_{IMAGE}	**0.4583**	**0.3306**	**0.3690**	**0.7211**	**0.4698**	**0.2604**	**0.2541**

All 116 fiducial spheres on the patient and phantom scans were successfully located and the fiducial marker configuration was validated in 100% of the cases. The average localization time of the human operator was 191.5 sec. The average localization time of the localization algorithm running on the i7-6700HQ CPU at 2.60GHz with 12GB RAM was 28.8 sec. In comparison with human operators, the localization algorithm reduces the time of the preoperative phase of marker localization by 84.96 %. After the implementation of the automatic localization algorithm, the human operators and medical personnel reported less stress during the preoperative planning phase of the surgery. In the cases when the patient's CT scan is taken just before the surgical procedure, the overall duration of the surgery is reduced by the average of 162.7 sec.



a) b)

Figure 9. Localized fiducial markers highlighted in a CT scan: a) x-shaped frame, b) Freely distributed markers

Based on the measurements done in clinical conditions on the patients and test phantoms, the localization algorithm has shown a considerably higher degree of accuracy and higher speed in comparison with human operators. Reliability in terms of successful localization of the fiducial marker has been 100% in the twenty tested cases. The use of the localization algorithm reduces the imaging and the registration error significantly. In a later upgrade of the RONNA system, the x-shaped frame was replaced with freely distributed fiducial markers that can be localized using the same algorithm. Both are shown in Figure 9.

5.2 Framework for the automated patient registration procedure

The main challenges associated with achieving the highest level of automation in the robotic neurosurgical patient registration procedure are:

- automation of the image space and the physical space localization
- solution to the problem of point-based correspondence between the two sets of localized fiducial points and the removal of potential outliers
- setup of the robot and the sensor framework for an automatic patient registration procedure
- validation of the robot system for an automatic patient registration procedure in the simulated and the actual clinical environment

At the start of the surgery, during the preparation phase of the RONNA procedure, the patient is brought to the OR. The robot is positioned near the patient and its position in relation to the patient is not known. In the OR, an OTS, i.e. an infrared stereo camera system with a large operating volume can be used for the localization of fiducial markers placed on the patient and on the robot. A fully automated patient registration procedure with a robot system using freely distributed fiducial markers requires automated localization procedures and an algorithm that can determine the corresponding point pairs between the image space and the physical space data sets.

The aim of PAPER 2 [43] was to measure and assess the medical applicability of a low-cost, lightweight industrial robot arm (Universal robot UR5) guided by the medically certified optical tracking system (Polaris Vicra) to positions registered from a CT scan. This research served for validating the technical capabilities of the OTS which was later used for the automation of the patient registration procedure in physical space. In the PAPER 3 [68], we introduced a complete solution for achieving the highest level of autonomy in the robotic neurosurgical patient registration procedure. To avoid the manual localization of fiducial markers in patient images, we use the automatic localization algorithm developed for the purpose of calculating the coordinates of each fiducial marker centre [55]. An OTS Polaris Spectra (NDI - Northern Digital Inc., Ontario, Canada) with a large field of view is used for the localization of fiducial markers attached to the patient and the robot in the OR. Once the OTS has a clear line of sight to the robot and the patient, the correspondence algorithm is used to determine point-pairs between the image space and the physical space.

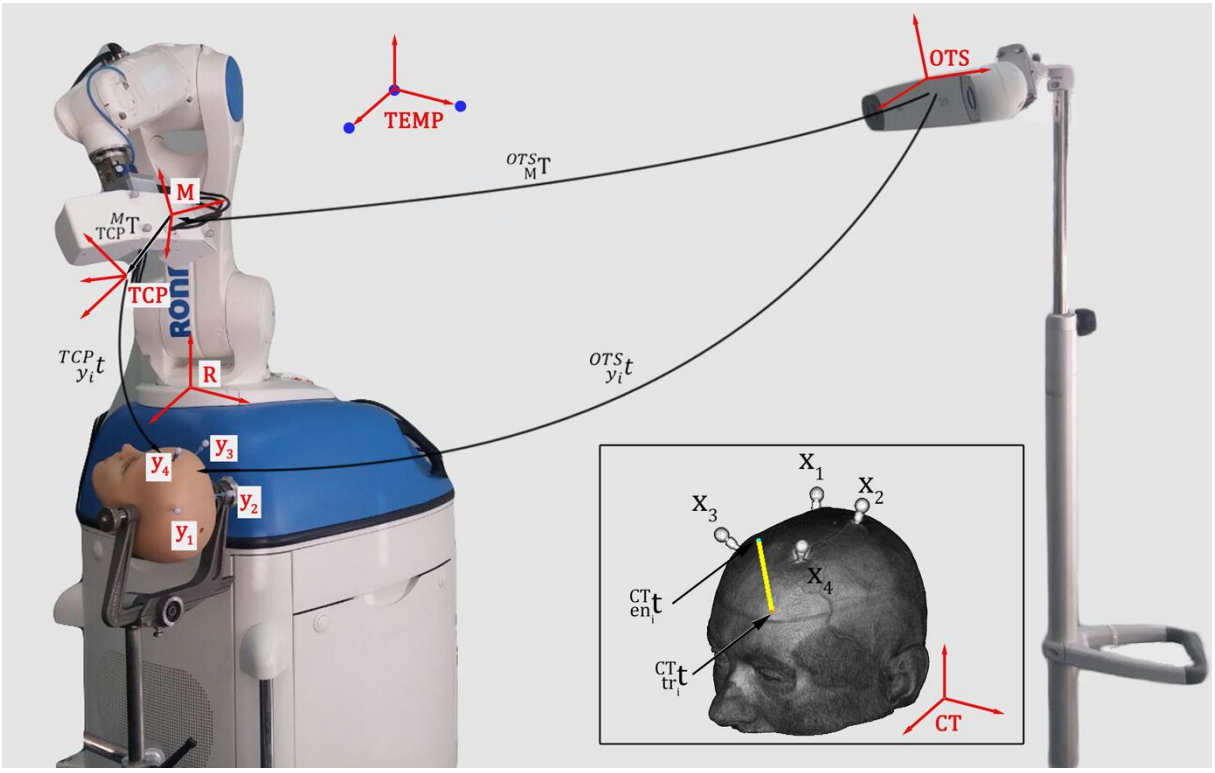


Figure 10. Coordinate systems and transformations used for achieving an automatic patient registration procedure

As shown in Figure 10., the OTS which retrieves the coordinates of the fiducial markers is used to attain the position and the orientation of the dynamic reference frame M mounted on the robot tool ($^{OTS}_{M}\mathbf{T}$) as well as the positions of the freely distributed fiducial markers $\{\boldsymbol{y}_i\}$ attached to the patient. M is retrieved in the OTS as $^{OTS}_{M}\mathbf{T}$, i.e. the position and orientation of the predefined configuration of individual fiducials attached to the robot tool. When the correspondence of points between the coordinate systems CT and OTS is established, we can calculate the position of the patient in the robot coordinate system R. After that, the robot automatically proceeds with the more precise re-localization of fiducial markers using RONNAstereo.

5.3 Correspondence algorithm

The x-shaped frame shown in Figure 2. a) is designed to carry four fiducial markers positioned at a unique distance from each other. During the first series of human clinical trials carried out in cooperation with a team of neurosurgeons from the University Hospital Dubrava, we noticed that the x-shaped frame implantation procedure proved to be impractical due to the frame size. An alternative was to replace the x-shaped frame with three or more individual self-drilling and self-tapping screws to which the retro-reflective spheres can be attached. For the problem of using fiducial markers placed at unknown distances to one-

another, we needed a registration algorithm that can compute the transformation between two point sets containing up to ten points each, with noise from the input devices and with a possibility of outlier points in both sets. As a solution to our specific problem, we have developed a novel correspondence algorithm. The algorithm uses a similarity matrix, with a known positional mean error and the standard deviations of the input data from the OTS and a CT scanner with the localization algorithm to validate successful point pairing and to remove potential outliers. This correspondence algorithm is presented in detail in PAPER 3 [68]. Example of the correspondence algorithm solution for a case with four fiducial markers and four randomly generated outlier points is shown in Figure 11.

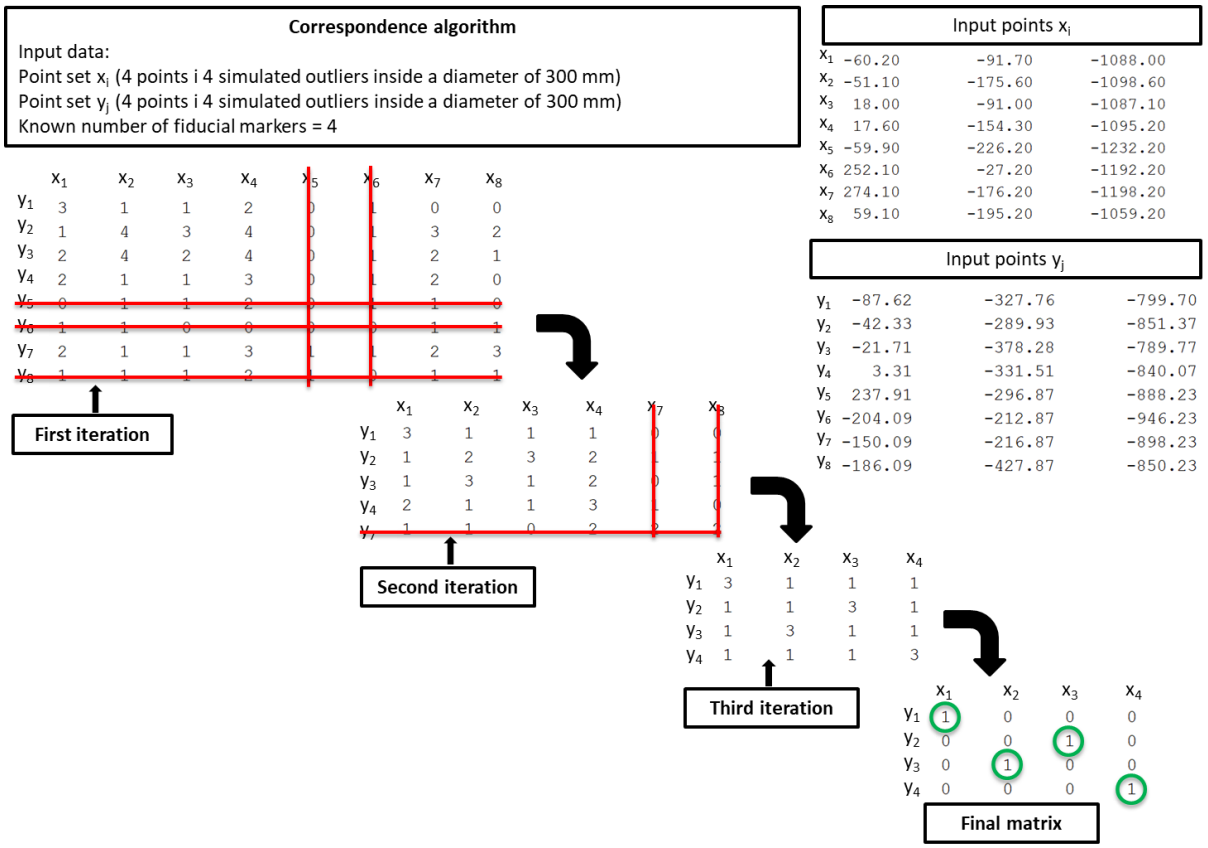
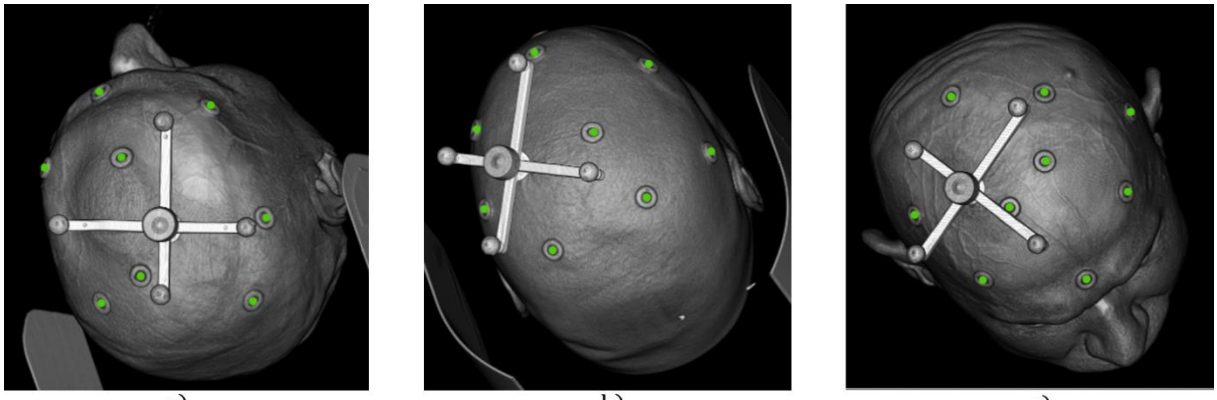


Figure 11. Example of the correspondence algorithm iterations

If one or more outlier points are found in any of the point sets, matrix cell values in rows and columns of those points will be lower than those of the fiducial points. Every row or column of the matrix that does not have at least one value that satisfies the condition is then removed as shown in the first and the second iteration in Figure 11. The algorithm iterates the procedure with a reduced number of points until it removes all the outliers or until the solution is confirmed as not being mathematically unique.

5.3.1 Testing of the correspondence algorithm in a simulated point environment

For the algorithm testing, we used the coordinates of eight adhesive fiducial markers manually attached to three patients by the neurosurgeon and localized in the CT scans. To compensate for the difference in the anatomy of a human head and the positioning of fiducial markers in different surgeries, we used uniform distribution inside a 10 mm radius sphere on the coordinates of every adhesive fiducial marker highlighted in Figure 12.



a) b) c)

Figure 12. Coordinates from adhesive fiducial markers (highlighted green) are used for testing the correspondence algorithm: a) Patient 1, b) Patient 2, c) Patient 3

The number of fiducial markers was three to eight. Randomly chosen fiducial markers were removed from the original set in every simulation with less than eight markers tested. The order of points in the second set was changed after the original set of points had been replaced. The noise was applied to both sets according to the calculated normal standard distribution of the input data (OTS in the physical space and localization algorithm in CT images), i.e. 0.56 mm in the original set and 0.17 mm in the second set. Furthermore, some tests were done without outlier points and some with one to four outlier points added to both sets. The positions of simulated outlier points were randomly chosen following a uniform distribution inside the sphere with a radius of 300 mm and with the centre defined as the centroid of all the fiducial markers. Ten thousand simulations were performed for each of the three patients. For each combination of the number of fiducial markers three to eight, and each number of added outlier points zero to four, we ran ten thousand simulations, resulting in a total of 900 000 tests. The algorithm was tested with the $e \in [1,6]$ mm parameter and 0.1 mm step. Where e is the value of the largest difference allowed between any two points that will be treated as a similarity point. There were three possible outcomes:

- Successful correspondence – correspondence of the exact number of points was found and the returned order of points was identical to the known order of points in both sets.

- Unsuccessful correspondence - due to large errors in the input data or an ambiguous solution.
- False-positive result - when the algorithm returned the correspondence but the order of points was not correct when checked with the known order of points in both sets.

Figure 13 shows the results of testing the correspondence algorithm (unsuccessful correspondence and the false-positive result).

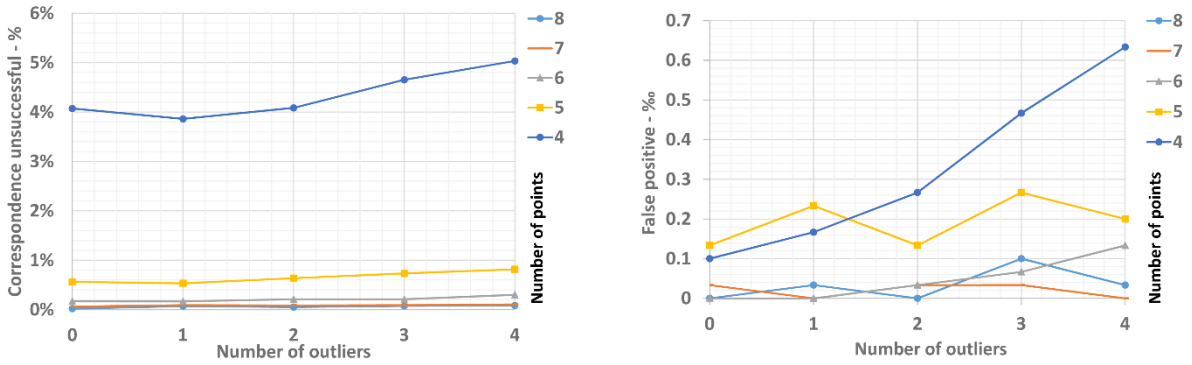


Figure 13. Results of testing the correspondence algorithm on simulated data: unsuccessful correspondence and the false-positive result

As expected, the correspondence algorithm has shown a higher percentage of success when a larger number of fiducial markers and a smaller number of outlier points were used. For five to eight fiducial markers and zero to four outlier points, the percentage of unsuccessful correspondence was between 0-0.81% and the number of false-positive results was between 0-0.026%. When only three or four fiducial markers were used, there was a higher chance of ambiguous solutions and hence a higher chance of unsuccessful correspondence and false-positive results. The unsuccessful correspondence for four fiducial markers was 3.86-5.03% and 7.98%-15.53% for three (not shown in Figure 13.). False-positive results for four fiducial markers amounted to 0.01-0.06% and 0.05-0.89% for three. Based on the test results, in the case when three or four fiducial markers are used, we suggest that there should be a physical template which would enable unique positioning distances in the patient preparation procedure.

5.3.2 Testing of the correspondence algorithm on clinical data

The purpose of these tests was to verify the reliability of the developed correspondence algorithm with the parameter $e \in [1,6]$ mm used on a real data set. The input data for the correspondence algorithm were the coordinates of the fiducial markers localized both in the physical and in the image space. In the image space, the fiducial markers were localized using the developed localization algorithm on CT scans of twelve patients taken after a brain biopsy

procedure and five CT scans of a laboratory phantom. In the physical space, the fiducial markers were localized using the Polaris Spectra OTS. We made 1415 measurements of the four fiducial markers mounted on the x-shaped frame. During the data acquisition stage, the x-shaped frame was constantly moved to ensure that different areas of the working volume are covered with the OTS. In Figures 14. and 15., the percentage of successful correspondences is shown in relation to the parameter *e* used in the algorithm.

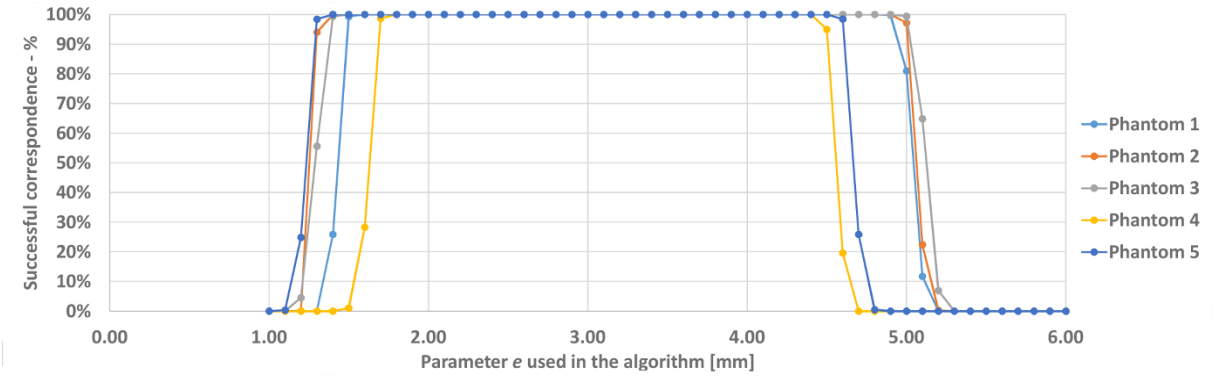


Figure 14. The success rate of the correspondence algorithm with the data from five CT scans of a laboratory phantom and OTS measurements

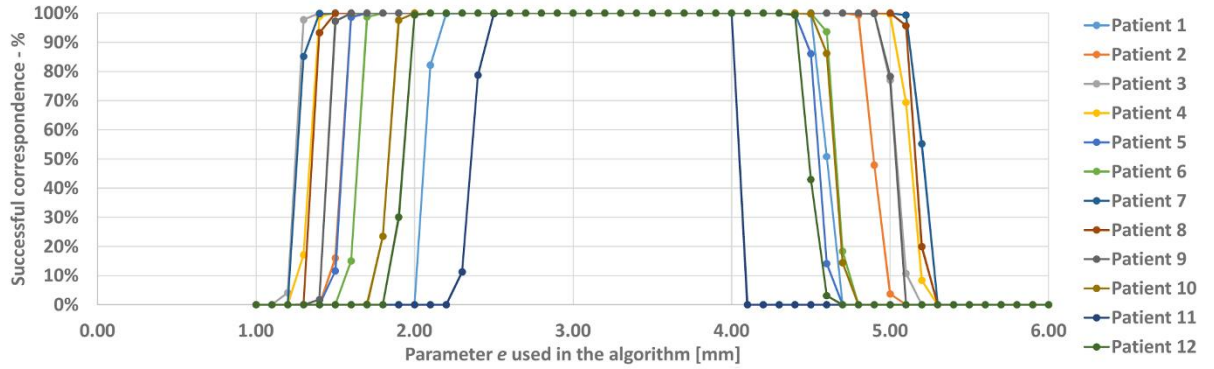


Figure 15. The success rate of the correspondence algorithm with the data from 12 patient CT scans and OTS measurements

In 24055 tests, the success rate was 100%. This can be contributed to the x-shaped marker which ensured that four fiducial markers were positioned at unique distances from one to the other. In Figures 14. and 15. one can note that the standard deviation of the errors in the phantom CT scans was lower than that in the patient CT scans and that the same OTS data was used in both cases. Consequently, there was a wider range of the applied parameter *e* that yields successful correspondence results. All the phantom CT scans had a 100% success rate for the $e \in [1.8,4.5]$ mm and all the patient CT scans for the $e \in [2.5,4]$ mm. There were no cases with unsuccessful correspondence or false-positive results in the specified interval of parameter *e* because the highest value of *e* was lower than those of the most similar distances between any two fiducial markers.

The successful point pairing between the patient image localization algorithm output and the OTS measurements ensures that there is no need for medical personnel to intervene in any phase of the patient registration procedure. In conclusion, the advantages of using freely distributed fiducial markers are:

- less invasiveness because of a smaller insertion diameter used for individual markers,
- better flexibility in choosing a position for fiducial markers on the patient's head in relation to the planned surgery target,
- simpler pre-operative procedure for implanting self-drilling and self-tapping screws,
- smaller registration error when individual fiducial markers are placed at larger distances,
- ability to use more than four fiducial markers if higher precision and accuracy are required,
- shorter distance from the fiducial markers to the surgical target.

5.4 Robot localization strategy and the accuracy of the neurosurgical robot system

The major challenges associated with the estimation of the robot positioning accuracy based on the registration error are:

- formulation of error analysis of a neurosurgical robot system,
- setting up of an objective measurement procedure
- isolation of the key parameters and determining their influence on the application accuracy of the neurosurgical robot system

Precise navigation of surgical instruments is one of the most important features of autonomous surgical robots. In PAPER 4 [18] we present laboratory phantom measurements that give evaluation of the RONNA positioning error for superficial (< 50 mm) and deep (50 mm to 120 mm) targets. In PAPER 5 [99], we introduced the concept of robot localization strategy in the patient registration procedure and analyse their influence on the overall application error. We defined the localization strategy as the utilization of specific robot approach angles, orientations and types of movement during the procedure of physical space fiducial marker localization and positioning to the target points. Robot tool pose is defined using a Cartesian coordinate system translation vector (x,y,z) and three orientation variables (α, β, γ) as a combination of Euler's angles with Z-Y-X convention. The starting hypothesis was that the magnitude of the registration error and the robot intrinsic error can be reduced by

utilizing localization strategies during the robot fiducial marker localization procedure and when positioning the robot tool at the planned target points. We have developed three localization strategies: neutral orientation strategy (NOS), orientation correction strategy (OCS) and joint displacement minimization strategy (JDMS). For the evaluation of the robot application accuracy, we performed laboratory phantom measurements for three different approaches to the robot localization procedure. In the registration procedure, we used two different registration methods and three, four, and five fiducial markers. More details on the localization strategies are available in the published paper [99].

Measurements results presented here are based on the data acquired for PAPER 5 [99]. Based on eight different laboratory phantom positions and ten target points for each phantom position, the average application errors for individual targets and all the strategies are shown in Table 4. In the NOS and the registration with three, four and five fiducial markers the average error was 1.571±0.256 mm, 1.397±0.283 mm and 1.327±0.274 mm, respectively. The NOS localizes the fiducial markers with the same neutral orientation and uses the same γ angle when positioning the robot tool to the target pose. Due to these features, a large difference in orientation is possible between the robot localization pose and the robot target pose. The result is a potentially bigger registration error, a bigger robot intrinsic error, and, consequently a bigger application error.

The overall average application error shown in Table 4 for the orientation correction strategy (OCS) and the registration with three, four, and five fiducial markers was 0.429±0.133 mm, 0.284±0.068mm, and 0.260±0.076 mm, respectively. OCS uses the same orientation when re-localizing the fiducial markers for every trajectory and when moving the robot tool to the target pose. The result of this approach is a smaller registration error and a smaller robot positioning error. Since the orientation of the robot tool does not change during the entire procedure we can state unequivocally that the errors in the calibration of the robot tool do not influence the registration error or the robot positioning error. Backlash error should be present in both the fiducial marker localization and the positioning at the target pose, the same as in the neutral orientation strategy. This strategy does not provide the optimum solution to the problem of either registration accuracy or robot positioning accuracy, but the accuracy in both cases is affected in such a way that it results in reduced errors.

The overall average application error shown in Table 4 for the joint displacement minimization strategy (JDMS) and the registration with four and five fiducial markers was

0.493±0.176 mm and 0.369±0.160 mm, respectively. JDMS uses different orientations when re-localizing every fiducial marker for every target pose, it also calculates and uses different sizes of the robot tool angle γ in the target pose. This approach should reduce the robot positioning error since the function calculates the orientation with which the minimal joint movement is necessary for the movements between the localization poses and each target pose. Furthermore, each localization pose and target pose is approached from the same joint direction to remove the influence of backlash. Since the localization of every fiducial marker is performed with a different robot tool orientation, potential errors in the calibration of the robot tool have a significant influence on the registration error.

Table 4. Measurement results of localization strategies

			Individual trajectory average error										Overall error		
			t_1	t_2	t_3	t_4	t_5	t_6	t_7	t_8	t_9	t_{10}	Average	Max	Min
NOS	No. of points used in the registration	3	1.645	1.665	1.925	1.586	1.705	1.378	1.374	1.383	1.444	1.602	**1.571**	2.245	1.081
		4	1.545	1.600	1.752	1.325	1.506	1.179	1.166	1.228	1.294	1.378	**1.397**	2.105	0.804
		5	1.466	1.533	1.667	1.244	1.452	1.120	1.095	1.174	1.233	1.291	**1.327**	2.007	0.770
OCS	No. of points used in the registration	3	0.346	0.380	0.616	0.556	0.338	0.289	0.388	0.320	0.473	0.583	**0.429**	0.773	0.201
		4	0.238	0.296	0.401	0.231	0.271	0.367	0.224	0.232	0.310	0.275	**0.284**	0.486	0.153
		5	0.210	0.260	0.338	0.167	0.292	0.397	0.231	0.221	0.265	0.222	**0.260**	0.442	0.128
JDMS	No. of points used in the registration	4	0.353	0.308	0.705	0.283	0.363	0.543	0.628	0.482	0.546	0.713	**0.493**	0.834	0.194
		5	0.254	0.247	0.575	0.151	0.323	0.310	0.517	0.372	0.393	0.548	**0.369**	0.691	0.016

The box plot in Figure 16 shows the measured application errors for all localization strategies and all numbers of fiducial markers used in the registration process. OCS showed the smallest average application error followed by JDMS. As expected, NOS had the biggest application error. For every localization strategy, the average application error was smaller if a larger number of fiducial markers were used in the registration. For OCS and JDMS the data were more closely distributed when a larger number of fiducial markers were used, while NOS had the smallest distribution when only three fiducial markers were used.

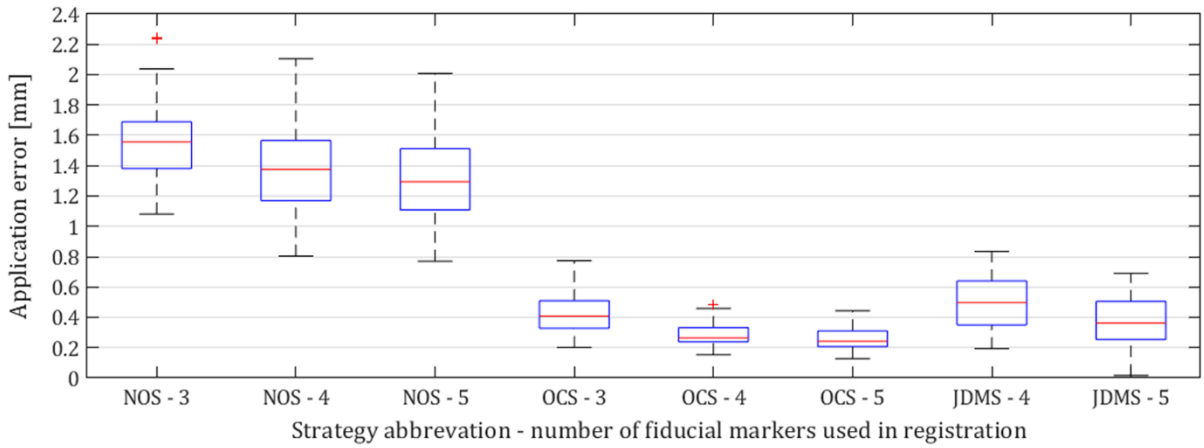


Figure 16. Measurement results of all localization strategies

The experimental results have shown that the impact of the robot localization strategy on the overall application accuracy of the neurosurgical robot system is significant. Based on the overall measurements results we can conclude that a larger number of fiducial markers used in the registration procedure improves the accuracy of a surgical robot system for every of the three robot localization strategies. In general, the measurement results in this study enable a good insight into the application accuracy of the RONNA system and offer a possibility of estimating the expected error in the positioning of the robot tool with respect to the type of markers, number of fiducial markers, localization method and localization strategies. The presented localization strategies can be used with any 6DOF (or 7DOF) revolute robot used in neurosurgical procedures to significantly reduce the application error regardless of the fact whether the robot has been previously calibrated or used with the nominal kinematic model supplied with the robot controller.

6 CONCLUSIONS AND FUTURE WORK

Research in the field of medical robotics, with application in neurosurgery, has attracted a widespread interest of the scientific and medical community and the general public because of the numerous benefits it provides. The main objective of this study was to contribute to the advancement of robotic application in neurosurgery, namely to research and improve the main components of the patient registration procedure in the neurosurgical robot system.

The main scientific contributions of this thesis are:

- an innovative algorithm developed for the recognition of localization features in CT patient images;
- a solution to the pair-point correspondence problem in the automation of the patient registration procedure;
- a model for the estimation of the robot positioning accuracy based on the registration error.

In this thesis, the developed fully automated image space localization algorithm uses a unique scientific approach which combines the existing machine vision algorithms, biomedical image filtration methods, and mathematical estimation methods. To our knowledge, there are not many studies and measurements that have been done for fully automated algorithms which search the CT image space for objects which are later localized in the physical space by a robot system. When our algorithm was compared to manual localization by human operators, the results showed improved accuracy, shorter localization time, and a 100% localization success rate. Furthermore, our localization algorithm uses retroreflective spheres (NDI passive spheres) which are commonly used for commercial neuronavigation systems (Medtronic's Stealth station, Brainlab neuronavigation etc.); therefore, it is available for comparison to other researchers in the field of biomedical image analysis and processing.

As a solution to the pair-point correspondence problem in the automatization of the patient registration procedure, a novel algorithm was developed; it is intended for finding the pair-point correspondence between freely distributed fiducial markers localized in the image space and the physical space by means of an OTS. The algorithm introduces a similarity matrix to

maximize the possibility of successful point pairing and to remove potential outlier points. Additionally, a framework for an automatic patient registration procedure using freely distributed fiducial markers within a robot application in neurosurgery is introduced. The proposed framework enables a fully automatic patient registration procedure when the robot arm and the patient are in the line of sight of the OTS. This solution greatly simplifies the localization procedure for the medical personnel and shortens the time needed for the operation.

A model for the estimation of the robot positioning accuracy based on the registration error is obtained from the laboratory phantom measurements and the surgical robot error analysis. The overall application accuracy of the robot system was measured using a different number of fiducials points used in the registration procedure and three different robot localization strategies in the physical space. The experimental results have shown that the impact of the robot localization strategy on the overall application accuracy of the neurosurgical robot system is significant. In general, the measurement results from this research enable medical personnel to get a good insight into the application accuracy of the RONNA system and into the possibility of estimating the expected error when positioning the robot tool in respect of the type of markers used, number of fiducial markers, localization method, depth of targets, and localization strategies.

In addition to the three main scientific contributions, this thesis also makes some important technical contributions. The following technical contributions are directly related to the robot system RONNA but also to the general procedures of spatial localization of patients and registration in neurosurgery:

- improved registration and application accuracy,
- shorter time needed for patient registration procedure (in both the image space and the physical space localization),
- automation of the entire patient registration procedure,
- introduction of freely distributed fiducial markers in the patient registration procedure,
- less invasiveness because of the smaller insertion diameter of individual markers,
- better flexibility in choosing a position of fiducial markers on the patient’s head in relation to the planned surgery target,
- the ability of the system to use more than four fiducial markers if higher precision, accuracy, and reliability are required,

- the measurement results from this research enable the medical personnel to get a good insight into the application accuracy of the RONNA system.

All of the listed improvements have been implemented in the RONNA system, tested in preclinical trials, and after that used in actual patient procedures [100].

In future research, we plan to implement markerless localization as an additional option in the patient registration procedure. According to the state of the art, markerless localization is less accurate than the extrinsic methods, so the greatest challenge would be to ensure similar accuracy to that presented in this thesis. Also, we plan to develop a new robot localization strategy as a combination of a modified and improved joint displacement minimization strategy, which should outperform the orientation correction strategy. The strategy will be implemented with a calibrated model of the robot to reduce errors caused by the robot tool calibration and to secure even smaller application errors.

7 LITERATURE

[1] K. Cleary and T. M. Peters, “Image-Guided Interventions: Technology Review and Clinical Applications,” Annual Review of Biomedical Engineering, vol. 12, no. 1, pp. 119–142, Jul. 2010.

[2] M. P. P. Vaghasiya and A. P. P. K. Gautam, “Image Registration Techniques: A Review,” International Journal Of Engineering And Computer Science, vol. 4, no. 2, pp. 10489–10492, Feb. 2015.

[3] F. P. M. Oliveira and J. M. R. S. Tavares, “Medical image registration: a review,” Computer Methods in Biomechanics and Biomedical Engineering, vol. 17, no. 2, pp. 73–93, Jan. 2014.

[4] C. R. Mascott, J.-C. Sol, P. Bousquet, J. Lagarrigue, Y. Lazorthes, and V. Lauwers-Cances, “Quantification of True In Vivo (Application) Accuracy in Cranial Image-guided Surgery: Influence of Mode of Patient Registration,” Operative Neurosurgery, vol. 59, p. ONS-146-ONS-156, Jul. 2006.

[5] R. Steinmeier, J. Rachinger, M. Kaus, O. Ganslandt, W. Huk, and R. Fahlbusch, “Factors influencing the application accuracy of neuronavigation systems,” Stereotactic and functional neurosurgery, vol. 75, no. 4, pp. 188–202, 2000.

[6] J. M. Henderson, K. L. Holloway, S. E. Gaede, and J. M. Rosenow, “The application accuracy of a skull-mounted trajectory guide system for image-guided functional neurosurgery,” Computer Aided Surgery, vol. 9, no. 4, pp. 155–160, Jan. 2004.

[7] F. Cardinale et al., “Stereoelectroencephalography: Surgical Methodology, Safety, and Stereotactic Application Accuracy in 500 Procedures,” Neurosurgery, vol. 72, no. 3, pp. 353–366, Mar. 2013.

[8] J. González-Martínez et al., “Technique, Results, and Complications Related to Robot-Assisted Stereoelectroencephalography:,” Neurosurgery, vol. 78, no. 2, pp. 169–180, Feb. 2016.

[9] G. Minchev et al., “A novel miniature robotic guidance device for stereotactic neurosurgical interventions: preliminary experience with the iSYS1 robot,” Journal of Neurosurgery, vol. 126, no. 3, pp. 985–996, Mar. 2017.

[10] M. Lefranc and D. Le Gars, “Robotic implantation of deep brain stimulation leads, assisted by intra-operative, flat-panel CT,” Acta Neurochirurgica, vol. 154, no. 11, pp. 2069–2074, Nov. 2012.

[11] Y. S. Kwoh, J. Hou, E. A. Jonckheere, and S. Hayati, “A robot with improved absolute positioning accuracy for CT guided stereotactic brain surgery,” IEEE Transactions on Biomedical Engineering, vol. 35, no. 2, pp. 153–160, Feb. 1988.

[12] M. S. Eljamel, “Validation of the PathFinderTM neurosurgical robot using a phantom,” The International Journal of Medical Robotics and Computer Assisted Surgery, vol. 3, no. 4, pp. 372–377, Dec. 2007.

[13] A. Bertelsen, J. Melo, E. Sánchez, and D. Borro, “A review of surgical robots for spinal interventions: A review of surgical robots for spinal interventions,” The International Journal of Medical Robotics and Computer Assisted Surgery, vol. 9, no. 4, pp. 407–422, Dec. 2013.

[14] T. Haidegger and I. J. Rudas, “From Concept to Market: Surgical Robot Development,” p. 39.

[15] D. Patel, “Dr. Patel performs groundbreaking robotic surgery in Switzerland.” Spine and Health institute.

[16] M. Lefranc and J. Peltier, “Evaluation of the ROSATM Spine robot for minimally invasive surgical procedures,” Expert Review of Medical Devices, vol. 13, no. 10, pp. 899–906, Oct. 2016.
[17] M. Lefranc et al., “The Impact of the Reference Imaging Modality, Registration Method and Intraoperative Flat-Panel Computed Tomography on the Accuracy of the ROSA® Stereotactic Robot,” Stereotactic and Functional Neurosurgery, vol. 92, no. 4, pp. 242–250, 2014.
[18] M. Švaco, B. Šekoranja, F. Šuligoj, J. Vidaković, B. Jerbić, and D. Chudy, “A Novel Robotic Neuronavigation System: RONNA G3,” Strojniški vestnik - Journal of Mechanical Engineering, vol. 63, no. 12, Dec. 2017.
[19] L. Chenin, J. Peltier, and M. Lefranc, “Minimally invasive transforaminal lumbar interbody fusion with the ROSATM Spine robot and intraoperative flat-panel CT guidance,” Acta Neurochirurgica, vol. 158, no. 6, pp. 1125–1128, Jun. 2016.
[20] W. Tian, H. Wang, and Y. Liu, “Robot-assisted Anterior Odontoid Screw Fixation: A Case Report: Robot-Assisted Odontoid Screw Fixation,” Orthopaedic Surgery, vol. 8, no. 3, pp. 400–404, Aug. 2016.
[21] W. Tian, “Robot-Assisted Posterior C1–2 Transarticular Screw Fixation for Atlantoaxial Instability: A Case Report,” SPINE, vol. 41, pp. B2–B5, Oct. 2016.
[22] C. Faria, C. Vale, M. Rito, W. Erlhagen, and E. Bicho, “A Simple Control Approach for Stereotactic Neurosurgery Using a Robotic Manipulator,” in CONTROLO 2016, vol. 402, P. Garrido, F. Soares, and A. P. Moreira, Eds. Cham: Springer International Publishing, 2017, pp. 397–408.
[23] E. Beretta, E. De Momi, F. Rodriguez y Baena, and G. Ferrigno, “Adaptive Hands-On Control for Reaching and Targeting Tasks in Surgery,” International Journal of Advanced Robotic Systems, vol. 12, no. 5, p. 50, May 2015.
[24] B. Jerbić, G. Nikolić, D. Chudy, M. Švaco, and B. Šekoranja, “Robotic application in neurosurgery using intelligent visual and haptic interaction,” International Journal of Simulation Modelling, vol. 14, no. 1, pp. 71–84, 2015.
[25] M. D. Comparetti, A. Vaccarella, I. Dyagilev, M. Shoham, G. Ferrigno, and E. De Momi, “Accurate multi-robot targeting for keyhole neurosurgery based on external sensor monitoring,” Proceedings of the Institution of Mechanical Engineers, Part H: Journal of Engineering in Medicine, vol. 226, no. 5, pp. 347–359, May 2012.
[26] S. Tovar-Arriaga, R. Tita, J. C. Pedraza-Ortega, E. Gorrostieta, and W. A. Kalender, “Development of a robotic FD-CT-guided navigation system for needle placement-preliminary accuracy tests,” The International Journal of Medical Robotics and Computer Assisted Surgery, vol. 7, no. 2, pp. 225–236, Jun. 2011.
[27] G. Deacon et al., “The Pathfinder image-guided surgical robot,” Proceedings of the Institution of Mechanical Engineers, Part H: Journal of Engineering in Medicine, vol. 224, no. 5, pp. 691–713, May 2010.
[28] G. Eggers et al., “Robot-Assisted Craniotomy,” min - Minimally Invasive Neurosurgery, vol. 48, no. 3, pp. 154–158, Jun. 2005.
[29] A. Burkart et al., “Precision of ACL tunnel placement using traditional and robotic techniques,” Computer Aided Surgery, vol. 6, no. 5, pp. 270–278, 2001.
[30] C. Faria, W. Erlhagen, M. Rito, E. De Momi, G. Ferrigno, and E. Bicho, “Review of Robotic Technology for Stereotactic Neurosurgery,” IEEE Reviews in Biomedical Engineering, vol. 8, pp. 125–137, 2015.
[31] J. A. Smith, J. Jivraj, R. Wong, and V. Yang, “30 Years of Neurosurgical Robots: Review and Trends for Manipulators and Associated Navigational Systems,” Annals of Biomedical Engineering, vol. 44, no. 4, pp. 836–846, Apr. 2016.

[32] S. Kantelhardt, N. Amr, and A. Giese, “Navigation and robot-aided surgery in the spine: historical review and state of the art,” Robotic Surgery: Research and Reviews, p. 19, Sep. 2014.
[33] A. Tan et al., “Robotic surgery: disruptive innovation or unfulfilled promise? A systematic review and meta-analysis of the first 30 years,” Surgical Endoscopy, vol. 30, no. 10, pp. 4330–4352, Oct. 2016.
[34] E. R. Cosman, Process of stereotactic optical navigation. Google Patents, 1997.
[35] A. Hussain, A. Malik, M. U. Halim, and A. M. Ali, “The use of robotics in surgery: a review,” International Journal of Clinical Practice, vol. 68, no. 11, pp. 1376–1382, Nov. 2014.
[36] G. P. Moustris, S. C. Hiridis, K. M. Deliparaschos, and K. M. Konstantinidis, “Evolution of autonomous and semi-autonomous robotic surgical systems: a review of the literature,” The International Journal of Medical Robotics and Computer Assisted Surgery, vol. 7, no. 4, pp. 375–392, Dec. 2011.
[37] G. Widmann, P. Schullian, M. Ortler, and R. Bale, “Frameless stereotactic targeting devices: technical features, targeting errors and clinical results,” The International Journal of Medical Robotics and Computer Assisted Surgery, vol. 8, no. 1, pp. 1–16, Mar. 2012.
[38] F. Cardinale et al., “A new tool for touch-free patient registration for robot-assisted intracranial surgery: application accuracy from a phantom study and a retrospective surgical series,” Neurosurgical Focus, vol. 42, no. 5, p. E8, May 2017.
[39] A. De Benedictis et al., “Robot-assisted procedures in pediatric neurosurgery,” Neurosurgical Focus, vol. 42, no. 5, p. E7, May 2017.
[40] G. Kronreif, W. Ptacek, M. Kornfeld, and M. Fürst, “Evaluation of robotic assistance in neurosurgical applications,” Journal of Robotic Surgery, vol. 6, no. 1, pp. 33–39, Mar. 2012.
[41] N. Gerber et al., “High-Accuracy Patient-to-Image Registration for the Facilitation of Image-Guided Robotic Microsurgery on the Head,” IEEE Transactions on Biomedical Engineering, vol. 60, no. 4, pp. 960–968, Apr. 2013.
[42] Fanle Meng, Hui Ding, and Guangzhi Wang, “A stereotaxic image-guided surgical robotic system for depth electrode insertion,” 2014, pp. 6167–6170.
[43] F. Šuligoj, B. Jerbić, M. Švaco, B. Šekoranja, D. Mihalinec, and J. Vidaković, “Medical applicability of a low-cost industrial robot arm guided with an optical tracking system,” in Intelligent Robots and Systems (IROS), 2015 IEEE/RSJ International Conference on, 2015, pp. 3785–3790.
[44] C.-C. Lin, H.-C. Lin, W.-Y. Lee, S.-T. Lee, and C.-T. Wu, “Neurosurgical robotic arm drilling navigation system: Robotic arm navigation system,” The International Journal of Medical Robotics and Computer Assisted Surgery, vol. 13, no. 3, p. e1790, Sep. 2017.
[45] H. Suenaga et al., “Vision-based markerless registration using stereo vision and an augmented reality surgical navigation system: a pilot study,” BMC Medical Imaging, vol. 15, no. 1, Dec. 2015.
[46] D. Á. Nagy, T. Haidegger, and Z. Yaniv, “A Framework for Semi-automatic Fiducial Localization in Volumetric Images,” in Augmented Environments for Computer-Assisted Interventions, Springer, 2014, pp. 138–148.
[47] M. Y. Wang, C. R. Maurer, J. M. Fitzpatrick, and R. J. Maciunas, “An automatic technique for finding and localizing externally attached markers in CT and MR volume images of the head,” IEEE Transactions on Biomedical Engineering, vol. 43, no. 6, pp. 627–637, 1996.
[48] Z. Yaniv, “Localizing spherical fiducials in C-arm based cone-beam CT,” Medical Physics, vol. 36, no. 11, p. 4957, 2009.

[49] Z. Yaniv, “Evaluation of spherical fiducial localization in C-arm cone-beam CT using patient data,” Medical Physics, vol. 37, no. 10, p. 5298, 2010.
[50] G. Fattori et al., “Automated Fiducial Localization in CT Images Based on Surface Processing and Geometrical Prior Knowledge for Radiotherapy Applications,” IEEE Transactions on Biomedical Engineering, vol. 59, no. 8, pp. 2191–2199, Aug. 2012.
[51] A. Isambert, G. Bonniaud, F. Lavielle, G. Malandain, and D. Lefkopoulos, “A phantom study of the accuracy of CT, MR and PET image registrations with a block matching-based algorithm,” Cancer/Radiothérapie, vol. 12, no. 8, pp. 800–808, Dec. 2008.
[52] J. Vidakovic, B. Jerbic, F. Suligoj, M. Svaco, and B. Sekoranja, “Simulation for Robotic Stereotactic Neurosurgery,” in DAAAM Proceedings, 1st ed., vol. 1, B. Katalinic, Ed. DAAAM International Vienna, 2016, pp. 0562–0568.
[53] L. Vajta and T. Juhasz, “The Role of 3D Simulation in the Advanced Robotic Design, Test and Control,” in Cutting Edge Robotics, V. Kordic, A. Lazinica, and M. Mer, Eds. Pro Literatur Verlag, Germany, 2005.
[54] B. Šekoranja, B. Jerbić, and F. Šuligoj, “Virtual surface for human-robot interaction,” Transactions of FAMENA, vol. 39, no. 1, pp. 53–64, 2015.
[55] F. Šuligoj, M. Švaco, B. Jerbić, B. Šekoranja, and J. Vidaković, “Automated Marker Localization in the Planning Phase of Robotic Neurosurgery,” IEEE Access, vol. 5, pp. 12265–12274, 2017.
[56] P. Gomes, “Surgical robotics: Reviewing the past, analysing the present, imagining the future,” Robotics and Computer-Integrated Manufacturing, vol. 27, no. 2, pp. 261–266, Apr. 2011.
[57] T. A. Mattei, A. H. Rodriguez, D. Sambhara, and E. Mendel, “Current state-of-the-art and future perspectives of robotic technology in neurosurgery,” Neurosurgical Review, vol. 37, no. 3, pp. 357–366, Jul. 2014.
[58] L. G. Brown, “A survey of image registration techniques,” ACM Computing Surveys, vol. 24, no. 4, pp. 325–376, Dec. 1992.
[59] H. Li and R. Hartley, “The 3D-3D Registration Problem Revisited,” in 2007 IEEE 11th International Conference on Computer Vision, Rio de Janeiro, Brazil, 2007, pp. 1–8.
[60] W. B. Heard, Rigid body mechanics: mathematics, physics and applications. Weinheim: Wiley-VCH, 2006.
[61] P. Tofts, Ed., Quantitative MRI of the brain: measuring changes caused by disease. Chichester, West Sussex ; Hoboken, NJ: Wiley, 2003.
[62] J. Ashburner and K. Friston, “Rigid Body Registration,” in Statistical Parametric Mapping, Elsevier, 2007, pp. 49–62.
[63] B. Bellekens, V. Spruyt, R. Berkvens, and M. Weyn, “A survey of rigid 3D point cloud registration algorithms,” in AMBIENT 2014: the Fourth International Conference on Ambient Computing, Applications, Services and Technologies, August 24-28, 2014, Rome, Italy, 2014, pp. 8–13.
[64] P. J. Besl, N. D. McKay, and others, “A method for registration of 3-D shapes,” IEEE Transactions on pattern analysis and machine intelligence, vol. 14, no. 2, pp. 239–256, 1992.
[65] O. Enqvist, “Correspondence problems in geometric vision,” Centre for Mathematical Sciences, Mathematics, Lund University, Lund, 2009.
[66] H. Lars Zimmer, “Correspondence Problems in Computer Vision,” Faculty of Mathematics and Computer Science, Saarland University, Saarbrucken, 2011.
[67] A. Parra Bustos and T.-J. Chin, “Guaranteed Outlier Removal for Point Cloud Registration with Correspondences,” IEEE Transactions on Pattern Analysis and Machine Intelligence, pp. 1–1, 2017.

[68] F. Šuligoj, B. Jerbić, M. Švaco, and B. Šekoranja, “Fully Automated Point-Based Robotic Neurosurgical Patient Registration Procedure,” International Journal of Simulation Modelling, vol. 17, no. 3, pp. 458–471, Sep. 2018.
[69] I. Soderkvist, “Using SVD for some fitting problems,” Technical note, p. 4.
[70] O. Sorkine-Hornung and M. Rabinovich, “Least-Squares Rigid Motion Using SVD,” Department of Computer Science, ETH Zurich, Technical note, p. 5, Jan. 2017.
[71] Z. Yaniv, “Rigid Registration,” in Image-Guided Interventions, T. Peters and K. Cleary, Eds. Boston, MA: Springer US, 2008, pp. 159–192.
[72] P. Markelj, D. Tomaževič, B. Likar, and F. Pernuš, “A review of 3D/2D registration methods for image-guided interventions,” Medical Image Analysis, vol. 16, no. 3, pp. 642–661, Apr. 2012.
[73] G. Eggers, J. Mühling, and R. Marmulla, “Image-to-patient registration techniques in head surgery,” International Journal of Oral and Maxillofacial Surgery, vol. 35, no. 12, pp. 1081–1095, Dec. 2006.
[74] P. S. Shiakolas, K. L. Conrad, and T. C. Yih, “On the Accuracy, Repeatability, and Degree of Influence of Kinematics Parameters for Industrial Robots,” International Journal of Modelling and Simulation, vol. 22, no. 4, pp. 245–254, Jan. 2002.
[75] Albert Nubiola, “Contribution to improving the accuracy of serial robots,” Montreal, 2014.
[76] Y. H. Andrew Liou, P. P. Lin, R. R. Lindeke, and H. D. Chiang, “Tolerance specification of robot kinematic parameters using an experimental design technique—the Taguchi method,” Robotics and Computer-Integrated Manufacturing, vol. 10, no. 3, pp. 199–207, Jun. 1993.
[77] C. Mavroidis, S. Dubowsky, P. Drouet, J. Hintersteiner, and J. Flanz, “A systematic error analysis of robotic manipulators: application to a high performance medical robot,” 1997, vol. 2, pp. 980–985.
[78] A. Nubiola and I. A. Bonev, “Absolute robot calibration with a single telescoping ballbar,” Precision Engineering, vol. 38, no. 3, pp. 472–480, Jul. 2014.
[79] L. Ma, P. Bazzoli, P. M. Sammons, R. G. Landers, and D. A. Bristow, “Modeling and calibration of high-order joint-dependent kinematic errors for industrial robots,” Robotics and Computer-Integrated Manufacturing, vol. 50, pp. 153–167, Apr. 2018.
[80] M. Švaco, B. Šekoranja, F. Šuligoj, and B. Jerbić, “Calibration of an Industrial Robot Using a Stereo Vision System,” Procedia Engineering, vol. 69, pp. 459–463, 2014.
[81] Y. Meng and H. Zhuang, “Self-Calibration of Camera-Equipped Robot Manipulators,” The International Journal of Robotics Research, vol. 20, no. 11, pp. 909–921, Nov. 2001.
[82] F. Boochs, R. Schutze, C. Simon, F. Marzani, H. Wirth, and J. Meier, “Increasing the accuracy of untaught robot positions by means of a multi-camera system,” in 2010 International Conference on Indoor Positioning and Indoor Navigation, Zurich, Switzerland, 2010, pp. 2010 International Conference on Indoor Positioning and Indoor Navigation (IPIN),1–9.
[83] J. Gonzalez-Martinez et al., “Robot-Assisted Stereotactic Laser Ablation in Medically Intractable Epilepsy: Operative Technique,” Neurosurgery, vol. 10, pp. 167–173, Jun. 2014.
[84] Q. H. Li, L. Zamorano, A. Pandya, R. Perez, J. Gong, and F. Diaz, “The Application Accuracy of the NeuroMate Robot—A Quantitative Comparison with Frameless and Frame-Based Surgical Localization Systems,” Computer Aided Surgery, vol. 7, no. 2, pp. 90–98, Jan. 2002.
[85] D. von Langsdorff, P. Paquis, and D. Fontaine, “In vivo measurement of the frame-based application accuracy of the Neuromate neurosurgical robot,” Journal of Neurosurgery, vol. 122, no. 1, pp. 191–194, Jan. 2015.

[86] M. Wang and Z. Song, “Improving target registration accuracy in image-guided neurosurgery by optimizing the distribution of fiducial points,” The International Journal of Medical Robotics and Computer Assisted Surgery, vol. 5, no. 1, pp. 26–31, Mar. 2009.
[87] R. R. Shamir, L. Joskowicz, and Y. Shoshan, “Fiducial Optimization for Minimal Target Registration Error in Image-Guided Neurosurgery,” IEEE Transactions on Medical Imaging, vol. 31, no. 3, pp. 725–737, Mar. 2012.
[88] M. Franaszek and G. S. Cheok, “Selection of fiducial locations and performance metrics for point-based rigid-body registration,” Precision Engineering, vol. 47, pp. 362–374, Jan. 2017.
[89] J. M. Fitzpatrick, “The role of registration in accurate surgical guidance,” Proceedings of the Institution of Mechanical Engineers, Part H: Journal of Engineering in Medicine, vol. 224, no. 5, pp. 607–622, May 2010.
[90] M. Perwög, Z. Bardosi, and W. Freysinger, “Experimental validation of predicted application accuracies for computer-assisted (CAS) intraoperative navigation with paired-point registration,” International Journal of Computer Assisted Radiology and Surgery, Aug. 2017.
[91] C. R. Maurer Jr, J. J. McCrory, and J. M. Fitzpatrick, “Estimation of accuracy in localizing externally attached markers in multimodal volume head images,” in Medical Imaging 1993, 1993, pp. 43–54.
[92] J. M. Fitzpatrick, J. B. West, and C. R. Maurer, “Predicting error in rigid-body point-based registration,” IEEE transactions on medical imaging, vol. 17, no. 5, pp. 694–702, 1998.
[93] J.-P. Kobler, J. Díaz Díaz, J. M. Fitzpatrick, G. J. Lexow, O. Majdani, and T. Ortmaier, “Localization accuracy of sphere fiducials in computed tomography images,” presented at the SPIE Medical Imaging, San Diego, California, USA, 2014.
[94] J. M. Fitzpatrick and J. B. West, “The distribution of target registration error in rigid-body point-based registration,” IEEE transactions on medical imaging, vol. 20, no. 9, pp. 917–927, 2001.
[95] R. R. Shamir and L. Joskowicz, “Geometrical analysis of registration errors in point-based rigid-body registration using invariants,” Medical Image Analysis, vol. 15, no. 1, pp. 85–95, Feb. 2011.
[96] J. M. Fitzpatrick, “Fiducial registration error and target registration error are uncorrelated,” presented at the SPIE Medical Imaging, Lake Buena Vista, FL, 2009, p. 726102.
[97] J. Liu, Y. Zhang, and Z. Li, “Improving the Positioning Accuracy of a Neurosurgical Robot System,” IEEE/ASME Transactions on Mechatronics, vol. 12, no. 5, pp. 527–533, Oct. 2007.
[98] M. A. Siebold, N. P. Dillon, R. J. Webster, and J. M. Fitzpatrick, “Incorporating target registration error into robotic bone milling,” presented at the SPIE Medical Imaging, Orlando, Florida, United States, 2015.
[99] F. Šuligoj, B. Jerbić, B. Šekoranja, J. Vidaković, and M. Švaco, “Influence of the Localization Strategy on the Accuracy of a Neurosurgical Robot System,” Transactions of FAMENA, vol. 42, no. 2, pp. 27–38, Jun. 2018.
[100] D. Dlaka et al., “Brain biopsy performed with the RONNA G3 system: a case study on using a novel robotic navigation device for stereotactic neurosurgery,” The International Journal of Medical Robotics and Computer Assisted Surgery, p. 1884, Dec. 2017.

8 CURRICULUM VITAE

Filip Šuligoj was born on March 25, 1986 in Zagreb, Croatia. In 2004, he finished high School, XI. Gimnazija, in Zagreb and started his studies at the Faculty of Mechanical Engineering and Naval Architecture (FMENA), University of Zagreb. He finished the undergraduate studies in mechanical engineering in 2008 and continued with the graduate studies in mechanical engineering, which he finished in 2009. From 2009 to 2013 he was employed at the Dalekovod proizvodnja d.o.o., and since2013, he has been employed at the Faculty of Mechanical Engineering and Naval Architecture, University of Zagreb, at the Department of Robotics and Production System Automation as a research assistant and a PhD student. In 2013, he received the "FESTO Prize for young researchers and scientists". He actively participated in research projects, "ACRON - A new concept of Applied Cognitive RObotics in clinical Neuroscience" and "Autonomous multiagent automatic assembly", and in technological projects, "Application of robots in neurosurgery", "RONNA - robotic neuronavigation", "NERO – neurosurgical robot", and "FAT - innovative Croatian solutions for the global automotive industry". He published 9 scientific papers in scientific journals and 8 scientific conference papers with international peer-review.

List of published scientific journals papers:

- Šuligoj, Filip; Jerbić, Bojan; Šekoranja, Bojan; Vidaković, Josip; Švaco, Marko Influence of the Localization Strategy on the Accuracy of a Neurosurgical Robot System. // Transactions of FAMENA, 42 (2018), 2; 27-38 doi:10.21278/tof.42203 (international peer review, article, scholarly)
- Dlaka, Domagoj; Švaco, Marko; Chudy, Darko; Jerbić, Bojan; Šekoranja, Bojan; Šuligoj, Filip; Vidaković, Josip; Almahariq, Fadi; Romić, Dominik Brain biopsy performed with the RONNA G3 system: a case study on using a novel robotic navigation device for stereotactic neurosurgery. // The International Journal of Medical Robotics and Computer Assisted Surgery, 14 (2017), 1; 10.1002/rcs.1884, 7 doi:10.1002/rcs.1884 (international peer review, article, scholarly)
- Vidaković, Josip; Jerbić, Bojan; Švaco, Marko; Šuligoj, Filip; Šekoranja Bojan Position planning for collaborating robots and its application in neurosurgery. // Znanstveno-

stručni časopis tehničkih fakulteta Sveučilišta u Osijeku, 24 (2017), 6; 1705-1711 (international peer review, article, scholarly)

- Švaco, Marko; Šekoranja, Bojan; Šuligoj, Filip; Vidaković, Josip; Jerbić, Bojan; Chudy, Darko; A novel robotic neuronavigation system: RONNA G3. // Strojniški vestnik, 63 (2017), 12; 725-735 doi:10.5545/sv-jme.2017.4649 (international peer review, article, scholarly)
- Šuligoj, Filip; Švaco, Marko; Jerbić, Bojan; Šekoranja, Bojan; Vidaković, Josip Automated marker localization in the planning phase of robotic neurosurgery. // IEEE Access, 5 (2017), 12265-12274 doi:10.1109/ACCESS.2017.2718621 (international peer review, article, scholarly)
- Šekoranja, Bojan; Jerbić, Bojan; Šuligoj Filip Virtual surface for human-robot interaction. // Transactions of FAMENA, 39 (2015), 1; 53-64 (international peer review, article, scholarly)
- Švaco, Marko; Jerbić, Bojan; Šuligoj Filip ARTgrid: A Two-Level Learning Architecture Based on Adaptive Resonance Theory. // Advances in Artificial Neural Systems, 2014 (2014), 1-9 doi:10.1155/2014/185492 (international peer review, article, scholarly)
- Švaco, Marko; Jerbić, Bojan; Šuligoj, Filip Autonomous robot learning model based on visual interpretation of spatial structures. // Transactions of FAMENA, 38 (2014), 4; 13-28 (international peer review, article, scholarly)
- Šuligoj, Filip; Jerbić, Bojan; Švaco, Marko; Šekoranja, Bojan Fully automated point-based robotic neurosurgical patient registration procedure. // International Journal of Simulation Modelling, (international peer review, article, accepted for publication in september 2018.)

List of published scientific conference papers:

- Švaco, Marko; Vitez, Nikola; Jerbić, Bojan; Šuligoj, Filip; Šekoranja, Bojan; Vidaković, Josip Experimental Evaluation of Parameters for Robotic Contouring Force Feedback Applications. // The International Conference Management of Technology – Step to Sustainable Production (MOTSP 2017) / Predrag Ćosić (ed.). Zagreb: Croatian Association for PLM, 2017. (poster, international peer review, full paper, scholarly)
- Švaco, Marko; Koren, Petar; Jerbić, Bojan; Vidaković, Josip; Šekoranja, Bojan; Šuligoj, Filip Validation of Three KUKA Agilus Robots for Application in Neurosurgery. // RAAD 2017: Advances in Service and Industrial Robotics / Ferraresi C., Quaglia G. (ed.).

Torino, Italija: Springer, 2017. pp. 996-1006 (lecture, international peer review, full paper, scholarly)

- Vidaković, Josip; Jerbić, Bojan; Šuligoj, Filip; Švaco, Marko; Šekoranja, Bojan SIMULATION FOR ROBOTIC STEREOTACTIC NEUROSURGERY. // Annals of DAAAM & Proceedings Mostar, Bosna i Hercegovina, 2016. pp. 562-568 (poster, international peer review, full paper, scholarly)
- Šuligoj, Filip; Jerbić, Bojan; Švaco, Marko; Šekoranja, Bojan; Mihalinec, Dominik; Vidaković, Josip Medical applicability of a low-cost industrial robot arm guided with an optical tracking system. // Intelligent Robots and Systems (IROS), 2015 IEEE/RSJ International Conference on Intelligent Robots and Systems Hamburg, Njemačka, 2015. (lecture, international peer review, full paper, scholarly)
- Jerbić, Bojan; Šuligoj, Filip; Švaco, Marko; Šekoranja, Bojan Robot Assisted 3D Point Cloud Object Registration. // Procedia Engineering 100 / Branko Katalinić (ed.). Vienna, 2014. pp. 847-852 (poster, international peer review, full paper, scholarly)
- Švaco, Marko; Šekoranja, Bojan; Šuligoj, Filip; Jerbić, Bojan Calibration of an Industrial Robot Using a Stereo Vision System. // Procedia Engineering 69 / Branko Katalinić (ed.). Zadar, Hrvatska, 2014. pp. 459-463 (poster, international peer review, full paper, scholarly)
- Šekoranja, Bojan; Bašić, Denis; Švaco, Marko; Šuligoj, Filip; Jerbić, Bojan Human-Robot Interaction Based on Use of Capacitive Sensors. // Procedia Engineering 69 / Branko Katalinic (ed.). Zadar, Hrvatska, 2014. pp. 464-468 (lecture, international peer review, full paper, scholarly)
- Šuligoj, Filip; Šekoranja, Bojan; Švaco, Marko; Jerbić, Bojan Object Tracking with a Multiagent Robot System and a Stereo Vision Camera. // Procedia Engineering 69 / Branko Katalinić (ed.). Zadar, Hrvatska, 2014. pp. 968-973 (lecture, international peer review, full paper, scholarly)

9 SUMMARY OF PAPERS

PAPER 1

F. Šuligoj, M. Švaco, B. Jerbić, B. Šekoranja, and J. Vidaković, "Automated Marker Localization in the Planning Phase of Robotic Neurosurgery," IEEE Access, vol. 5, pp. 12265–12274, 2017.

Accurate patient registration is a critical issue in medical image-guided interventions. The neurosurgical robot system RONNA (RObotic Neuro-NAvigation) uses four retro-reflective spheres on four markers attached to the patient's cranial bone for patient registration in the physical and the image space. In this paper, a newly developed algorithm for the automatic localization of spherical fiducials in CT scans is presented and clinically evaluated. This localization algorithm uses a unique approach which combines machine vision algorithms, biomedical image filtration methods, and mathematical estimation methods. The performance of the localization algorithm was evaluated in comparison with four skilled human operators. The measurements were based on twelve patient and eight lab phantom CT scans. Results: The localization error of the algorithm in comparison with the human readings was smaller by 49.29% according to the ground truth estimation and by 45.91% according to the intra-modal estimation. Localization processing time was reduced by 84.96%. Reliability in terms of successful localization of the fiducial marker was 100% for twenty different test samples containing a total of 116 spherical fiducials.

In the context of doctoral thesis hypothesis and contribution, the newly developed algorithm provides fully automated and accurate machine vision-based patient localization for the neurosurgical clinical application of the robotic system RONNA.

The localization algorithm presented in this paper was developed and programmed by Šuligoj, while Švaco programmed the pixel-to-Cartesian space conversion and Hounsfield scale filtering segment. Measurement framework and calculations were set up by Šuligoj and conducted in cooperation with Šekoranja, Vidaković and Švaco. The paper was written by Šuligoj and reviewed by Jerbić, Švaco, Šekoranja and Vidaković.

PAPER 2

F. Šuligoj, B. Jerbić, M. Švaco, B. Šekoranja, D. Mihalinec, and J. Vidaković, "Medical applicability of a low-cost industrial robot arm guided with an optical tracking system," in Intelligent Robots and Systems (IROS), 2015 IEEE/RSJ International Conference on, 2015, pp. 3785–3790.

The aim of this paper was to measure and assess the medical applicability of a low-cost, lightweight industrial robotic arm (Universal robot UR5) guided by a medically certified optical tracking system (Polaris Vicra) to positions registered from a CT scan. The technical setup, measuring devices, device communication, and robot control based on the OTS feedback are described. Robot intrinsic accuracy, CT scan accuracy and the accuracy of two methods of robot tool positioning with the aid of optical tracking system (OTS) are measured.

This research served as an introduction to and the testing of system accuracy when using an OTS for robot navigation. The measurements and the technical setup contributed to the later research where a fully automatic framework for patient registration was developed.

In this paper, the technical and experiment setup were programmed and organized by Šuligoj. Mihalinec carried out the robot and OTS measurements in the physical space and Vidaković CT measurements in the image space. The paper was written by Šuligoj and reviewed by Jerbić, Šekoranja and Švaco.

PAPER 3

F. Šuligoj, B. Jerbić, M. Švaco, and B. Šekoranja, “Fully Automated Point-Based Robotic Neurosurgical Patient Registration Procedure,” International Journal of Simulation Modelling, vol. 17, no. 3, pp. 458–471, Sep. 2018.

In this study, we have introduced a framework for an automatic patient registration procedure using freely distributed fiducial markers within a robot application in neurosurgery. The localization procedures in the image space and in the physical space are fully automated. We have developed a novel algorithm for finding the point pair correspondence between freely distributed fiducial markers in the image and in the physical space. The algorithm introduces a similarity matrix to maximize the possibility of successful point pairing and to remove the potential outlier points. The correspondence algorithm has been tested in 900,000 computer simulations and also on the real data from five laboratory phantom CT scans and twelve clinical patient CT scans, which were paired with 1415 readings captured with an optical tracking system. The testing of simulated point scenarios showed that the correspondence algorithm has a higher percentage of success when a larger number of fiducial markers and a lower number of outlier points were present. In 24055 tests on the clinical data there was a 100% success rate.

This research is directly connected to the doctoral thesis second hypothesis and second contribution. The study focuses on the development and testing of the newly developed correspondence algorithm and a framework for an automatic patient registration procedure using freely distributed fiducial markers within a robot application in neurosurgery.

In this paper, the correspondence algorithm, the framework and the simulations were developed by Šuligoj, while Jerbić and all the other authors participated in the planning of the main system components. Šuligoj planned and carried out the experiments. The paper was written by Šuligoj and Švaco wrote the state-of-the-art section. The paper was reviewed by Jerbić, Švaco, Šekoranja and Vidaković.

PAPER 4

M. Švaco, B. Šekoranja, F. Šuligoj, J. Vidaković, B. Jerbić, and D. Chudy, "A Novel Robotic Neuronavigation System: RONNA G3," Strojniški vestnik - Journal of Mechanical Engineering, vol. 63, no. 12, Dec. 2017.

This paper presents a novel robotic neuronavigation system, RONNA G3, developed for frameless stereotactic navigation based on standard industrial robots. The basic version of the RONNA G3 system has three main components: a robotic arm mounted on a universal mobile platform, a planning system, and a navigation system. We have developed a stereovision localization device (RONNAstereo) which can be attached to the robot end effector for accurate non-contact localization of the patient in the operating room. RONNAstereo has two infrared (IR) cameras with macro lenses aligned at a 55° angle in the same plane. We have evaluated the application accuracy of the RONNA G3 system in a phantom study with two different registration methods. The first registration method involves a rigid fiducial marker with four retroreflective spheres (spherical fiducials). The second method uses freely distributed individual spherical fiducials mounted on single bone screws. We have evaluated the RONNA G3 positioning error for superficial (<50 mm) and deep (50 - 120 mm) targets. The mean target positioning error (TPE) of the RONNA G3 system for superficial and deep targets was 0.43 mm (interquartile range 0.22 - 0.60 mm) and 0.88 mm (interquartile range 0.66 – 1.10 mm), respectively. Taking into account the positioning errors from the phantom trials, we have prepared a system for clinical trials which are currently in progress.

This paper gives an overview of all functionalities of RONNA and the clinical workflow. The paper also presents important clinical accuracy measurements for superficial and deep targets. The importance of this paper for the doctoral thesis is that it gives information about the complete system and the patient registration procedure. It also gives important metrics that can be used by the medical personnel when planning future operations.

For the purpose of this study, the complete RONNA system was developed by Jerbić, Švaco, Šekoranja, Šuligoj, and Vidaković, adopting practical medical suggestions made by Chudy. The measurements were organized and conducted by Vidaković and Šekoranja. The paper was written by all the authors, with Šuligoj writing the segments related to the patient registration procedure. The paper was reviewed by Jerbić and Chudy.

PAPER 5

F. Šuligoj, B. Jerbić, B. Šekoranja, J. Vidaković, and M. Švaco, "Influence of the Localization Strategy on the Accuracy of a Neurosurgical Robot System," Transactions of FAMENA, vol. 42, no. 2, pp. 27–38, Jun. 2018.

In this paper, we introduced the concept of robot localization strategy and analysed its influence on the overall application error of a robot system for frameless stereotactic neurosurgery, RONNA. The newly developed localization strategies presented in this paper are neutral orientation strategy (NOS), orientation correction strategy (OCS), and joint displacement minimization strategy (JDMS). To evaluate the robot positioning performance using the three localization strategies, we performed laboratory phantom measurements using a different number of fiducial markers in the registration procedure. When three, four and five fiducial markers were used the application error for NOS was 1.571±0.256 mm, 1.397±0.283 mm, and 1.327±0.274 mm, and for OCS 0.429±0.133 mm, 0.284±0.068mm, and 0.260±0.076 mm, respectively. The application error for JDMS was 0.493±0.176 mm for four and 0.369±0.160 mm for five fiducial markers.

In this paper, the third contribution to the doctoral thesis is given. The measurement results in this study enable a good insight into the application accuracy of the RONNA system and a possibility of estimating the expected error when positioning the robot tool in respect with the type of markers, number of fiducial markers, localization method and localization strategies.

In this paper, the term localization strategy was introduced and developed by Šuligoj. Šuligoj programmed the JDM strategy and Švaco and Šekoranja the OC and NO strategies. The measurement setup was programmed by Šekoranja, Vidaković, and Šuligoj, while the measurements were planned and conducted by Šuligoj. The paper was written by Šuligoj and reviewed by Jerbić, Šekoranja and Švaco.

10 APPENDIX

PAPER 1

PAPER 2

PAPER 3

PAPER 4

PAPER 5